

Heavy-Tailed Loss Frequencies from Mixtures of Negative Binomial and Poisson Counts

Jiansheng Dai,^{*} Ziheng Huang,[†] Michael R. Powers,[‡] and Jiaxin Xu[§]

November 8, 2022

Abstract

Heavy-tailed random variables have been used in insurance research to model both loss frequencies and loss severities, with substantially more emphasis on the latter. In the present work, we take a step toward addressing this imbalance by exploring the class of heavy-tailed frequency models formed by continuous mixtures of Negative Binomial and Poisson random variables. We begin by defining the concept of a calibrative family of mixing distributions (each member of which is identifiable from its associated Negative Binomial mixture), and show how to construct such families from only a single member. We then introduce a new heavy-tailed frequency model – the two-parameter ZY distribution – as a generalization of both the one-parameter Zeta and Yule distributions, and construct calibrative families for both the new distribution and the heavy-tailed two-parameter Waring distribution. Finally, we pursue natural extensions of both the ZY and Waring families to a unifying, four-parameter heavy-tailed model, providing the foundation for a novel loss-frequency modeling approach to complement conventional GLM analyses. This approach is illustrated by application to a classic set of Swedish commercial motor-vehicle insurance loss data.

Keywords: Loss frequency; heavy tail; continuous mixture; identifiability; calibrative family; Negative Binomial; Poisson.

1 Introduction

Let \mathcal{H}_D denote the family of heavy-tailed discrete random variables, $X \in \{0, 1, 2, \dots\}$, characterized by probability mass function (PMF) $f_X(x) > 0$, for which $E_X[X^\delta] = \lim_{n \rightarrow \infty} \sum_{x=0}^n x^\delta f_X(x) = \infty$ for some real-valued $\delta \in (0, \infty)$, and let \mathcal{H}_C denote the corresponding family of heavy-tailed continuous random variables, $Y \in (0, \infty)$, with probability density function (PDF) $f_Y(y) > 0$, such that $E_Y[Y^\delta] = \lim_{t \rightarrow \infty} \int_0^t y^\delta f_Y(y) dy = \infty$ for some positive real δ . Although models from both families have been employed

^{*}WizardQuant Investment Management; email: daiball@yeah.net.

[†]Sixie Capital Management; email: huangziheng1996@126.com.

[‡]Corresponding author; B306 Lihua Building, Department of Finance, School of Economics and Management, and Schwarzman College, Tsinghua University, Beijing, China 100084; email: powers@sem.tsinghua.edu.cn.

[§]Department of Finance, School of Economics and Management, Tsinghua University; email: xujx.18@sem.tsinghua.edu.cn.

in the insurance literature, substantially more attention has been paid to the latter than the former. This difference may be entirely warranted, simply because individual and total loss amounts (severities and total losses, respectively) are more likely to be characterized by heavy tails than are loss counts (frequencies). However, another consideration – which we believe explains at least part of the difference – is that the distributions in \mathcal{H}_C are more familiar and/or more tractable than those in \mathcal{H}_D . A principal aim of the present work is to draw greater attention to heavy-tailed frequency distributions by exploring the class of heavy-tailed frequency models formed by continuous mixtures of Negative Binomial (and therefore Poisson) random variables.

Two of the simplest and best-known sub-families of \mathcal{H}_D are:

(1) $X|s \sim \text{Zeta}(s)$, with

$$f_{X|s}^{(Z)}(x) = \frac{(x+1)^{-s}}{\zeta(s)}, \quad (1)$$

for $s \in (1, \infty)$, where $\zeta(s) = \sum_{x=0}^{\infty} (x+1)^{-s}$ denotes the Riemann zeta function; and

(2) $X|b \sim \text{Yule}(b)$, with

$$f_{X|b}^{(Y)}(x) = bB(x+1, b+1), \quad (2)$$

for $b \in (0, \infty)$, where $B(u, w) = \frac{\Gamma(u)\Gamma(w)}{\Gamma(u+w)}$ denotes the beta function.¹

Both of these distributions have been proposed to model loss frequencies,² and they possess comparable properties, including asymptotically equivalent tails when $b = s - 1$. Nevertheless, the similarities and differences of the two mathematical models have not been analyzed closely in the literature. In particular, although it is well known that the Yule distribution (as a special case of the three-parameter Generalized Waring distribution) can be expressed as a continuous mixture of Negative Binomial random variables (as shown in Subsection 3.1 below), no comparable result existed for the Zeta distribution until very recently (see Dai, Huang, Powers, and Xu, 2021). Therefore, these two types of random variables afford a natural starting point for the present study.

Following a brief overview of the use of heavy-tailed random variables in insurance in Section 2, we explore the formation of heavy-tailed frequencies from continuous mixtures of Negative Binomial and Poisson random variables. In Section 3, we define the concept of a calibrative family of mixing distributions (each member of which is identifiable from its associated Negative Binomial mixture), and show how to construct such families from only a single member. Then, in Section 4, we introduce a new heavy-tailed

¹The Zeta(s) and Yule(b) distributions often are defined on the sample space $x \in \{1, 2, 3, \dots\}$ rather than $x \in \{0, 1, 2, \dots\}$. However, we work with the latter characterization both because it matches the sample space of the Poisson(λ) distribution and because it is the more commonly used formulation in insurance applications.

²See, for example, Doray and Luong (1995) for Zeta applications and Irwin (1968) for Yule applications (as a special case of the Generalized Waring distribution).

frequency model – the two-parameter ZY distribution – as a generalization of both the one-parameter Zeta and Yule distributions, and construct calibrative families for both the new distribution and the heavy-tailed two-parameter Waring distribution, investigating their similarities and differences. Finally, we pursue natural extensions of both the ZY and Waring families to a unifying, four-parameter heavy-tailed model, providing the foundation for a novel loss-frequency modeling approach to complement conventional GLM analyses. This approach is illustrated by application to a set of historical Swedish commercial motor-vehicle insurance loss data.

2 Heavy-Tailed Random Variables in Insurance

An obvious place to look for applications of heavy-tailed loss models is among the damages caused by nature’s most destructive forces: wind, storms, tidal waves, and earthquakes. Indeed, it is widely recognized that such physical forces exhibit magnitudes that are well modeled by power laws; and the values of real property – houses, buildings, factories, etc. – also tend to follow such distributions (in much the same way as personal income and wealth). (See, e.g., Newman, 2005.)

Interestingly, however, heavy-tailed probability models rarely play an explicit role in contemporary property-catastrophe loss forecasting. This is not because they are inconsistent with historical data, but rather because today’s insurance industry favors methods relying heavily on engineering-based simulation, in which the numbers of properties damaged (frequencies), and their respective insured values, are generated implicitly through random scenarios. The sizes of individual losses (severities), then are drawn from (bounded) Beta distributions whose scale factors (upper bounds) are given by the respective insured values. Finally, the resulting total-loss random variables – although likely to be heavy-tailed in theory – are characterized by (bounded) empirical distributions.

As a consequence of such practices, the most common applications of heavy-tailed models do not involve physically forceful loss processes, but rather the heterogeneity of frequencies and severities associated with more mundane perils. This heterogeneity can arise from any of a number of sources, running the gamut from simple to complex. At the former end of the spectrum, it is easy to envision a commercial insurance company whose overall loss frequency consists of a mixture of individual policyholder frequencies, the means of which follow a power law. At the latter end, one might imagine an insurance company that, because of underwriting problems, begins to cover policyholders whose expected frequencies and/or severities follow a heavy-tailed distribution.

Instructively, even the simplest frequency or severity models can be converted easily into heavy-tailed

random variables by an elementary transformation attributable to risk heterogeneity.

For example, suppose a commercial policyholder's medical-expense loss frequency is given by a Geometric (p) random variable; that is, $X | p \sim f_{X|p}^{(G)}(x) = (1-p)p^x$, $x \in \{0, 1, 2, \dots\}$.³ Suppose further that the mean frequency, $\mu_X = E_{X|p}[X] = \frac{p}{1-p}$, varies with the policyholder's number of employees, and follows a Pareto 2 ($\alpha = 1, \theta = 1$) distribution with $f_{\mu|\alpha=1, \theta=1}^{(P2)}(\mu) = \frac{1}{(\mu+1)^2}$, $\mu \in (0, \infty)$. In that case, $p|a, b = 1 \sim \text{Beta}(a, b = 1) \equiv \text{Uniform}(0, 1)$, and the unconditional medical-expense frequency, X , is a Yule ($b = 1$) random variable with $f_{X|b=1}^{(Y)}(x) = \frac{1}{(x+1)(x+2)}$.

Alternatively, consider a personal-lines policyholder whose liability loss severity is given by an Exponential (λ) random variable, such that $Y | \lambda \sim f_{Y|\lambda}^{(E)}(y) = \lambda e^{-\lambda y}$, $y \in (0, \infty)$. Now assume that, because of classification errors and/or information deficiencies, the mean severity, $\mu_Y = E_{Y|\lambda}[Y] = \frac{1}{\lambda}$, follows an Inverse Exponential (θ) distribution with $f_{\mu|\theta}^{(IE)}(\mu) = \frac{\theta}{\mu^2} e^{-\theta/\mu}$, $\mu \in (0, \infty)$. In this case, $\lambda|\theta \sim \text{Exponential}(\theta)$, and the unconditional liability severity, Y , is a Pareto 2 ($\alpha = 1, \theta$) random variable with $f_{Y|\alpha=1, \theta}^{(P2)}(y) = \frac{\theta}{(y+\theta)^2}$.

As noted in the Introduction, heavy-tailed frequency models are much less commonly used in actual practice than heavy-tailed severity models. This does not necessarily mean that heavy-tailed frequencies are rare; in fact, we would argue that, because of heterogeneous risk levels, heavy-tailed frequencies are quite common. Rather, the dearth of such models is likely explained – at least in part – by a lack of familiar and tractable heavy-tailed discrete distributions, and a concomitant shortage of related mathematical analysis. (See, e.g., Karlis, 2005.) The present work is intended as a step toward addressing these issues.

3 Heavy-Tailed Frequency Models

3.1 Mixtures of Negative Binomial Counts

We begin by focusing on members of \mathcal{H}_D that are formed as mixtures of Negative Binomial (r, p) random variables by treating the r parameter as fixed, and the p parameter as a continuous random variable, $p|\boldsymbol{\eta} \sim f_{p|\boldsymbol{\eta}}(p) > 0$, $p \in (0, 1)$, where $\boldsymbol{\eta}$ denotes a vector of distributional parameters. To that end, let $X | r, p \sim \text{Negative Binomial}(r, p)$ with $f_{X|r, p}^{(NB)}(x) = \frac{\Gamma(x+r)}{\Gamma(r)\Gamma(x+1)} (1-p)^r p^x$, $x \in \{0, 1, 2, \dots\}$, for $r \in (0, \infty)$ and

³We parameterize the Geometric (p) \equiv Negative Binomial ($r = 1, p$) distribution – and later the general Negative Binomial (r, p) distribution – using the symbol p to represent the probability of a “failure” prior to the r^{th} “success” (as opposed to the probability of a success, as is more common). This is because the present parameterization facilitates certain mathematical derivations (see, e.g., Subsection A.1 of the Appendix) by permitting the product $(1-p)p^x$ to be broken into two additive components, $p^x - p^{x+1}$ (which cannot be done with the alternative product, $p(1-p)^x$).

$p \in (0, 1)$, and consider the family of mixing PDFs, $\mathcal{M}_{\text{NB}}^{\mathcal{H}}$, such that $f_{p|\boldsymbol{\eta}}(p) \in \mathcal{M}_{\text{NB}}^{\mathcal{H}} \implies$

$$X|r, \boldsymbol{\eta} \sim f_{X|r, \boldsymbol{\eta}}(x) = \int_0^1 \frac{\Gamma(x+r)}{\Gamma(r)\Gamma(x+1)} (1-p)^r p^x f_{p|\boldsymbol{\eta}}(p) dp \quad (3)$$

is a member of \mathcal{H}_{D} .

For simplicity, we will limit membership in $\mathcal{M}_{\text{NB}}^{\mathcal{H}}$ to differentiable PDFs that do not oscillate asymptotically as p approaches either 0 or 1 (i.e., $f'_{p|\boldsymbol{\eta}}(p)$ is well defined everywhere on $(0, 1)$, and changes sign only a finite number of times on this interval). The following result provides necessary and sufficient conditions for a mixing PDF to be a member of $\mathcal{M}_{\text{NB}}^{\mathcal{H}}$.

Theorem 1: The following three statements are equivalent:

- (a) $f_{p|\boldsymbol{\eta}}(p) \in \mathcal{M}_{\text{NB}}^{\mathcal{H}}$;
- (b) $\lim_{p \rightarrow 1^-} f_{p|\boldsymbol{\eta}}(p) (1-p)^{-\delta+1} = L > 0$ for some $\delta \in (0, \infty)$; and
- (c) $\lim_{p \rightarrow 1^-} \frac{\ln(f_{p|\boldsymbol{\eta}}(p))}{\ln(1-p)} < \infty$.

Proof: See Subsection A.1 of the Appendix.

Statement (b) of the above theorem means that $f_{p|\boldsymbol{\eta}}(p)$ follows an inverse power law in the limit as $p \rightarrow 1^-$, which is consistent with the restriction that $f'_{p|\boldsymbol{\eta}}(p)$ changes sign only a finite number of times on $(0, 1)$. If we initially had permitted asymptotically oscillating functional forms for $f_{p|\boldsymbol{\eta}}(p)$, then condition (b) would represent a narrowing of the set of possible PDFs. The value of statement (c) comes from its parsimony; that is, the condition can be expressed without reference to any specific parameter $\delta \in (0, \infty)$.

One well-studied member of $\mathcal{M}_{\text{NB}}^{\mathcal{H}}$ is the Generalized Beta 1 (a, b, c) PDF, $f_{p|a,b,c}^{(\text{GB1})}(p) = \frac{c}{\text{B}(a,b)} p^{ca-1} (1-p^c)^{b-1}$, for $a, b, c \in (0, \infty)$. This distribution, defined by McDonald (1984) with an arbitrary positive scale factor, contains Beta $(a, b) \equiv$ Generalized Beta 1 $(a, b, c = 1)$ and Kumaraswamy $(b, c) \equiv$ Generalized Beta 1 $(a = 1, b, c)$ as special cases. Although we are not aware of any comprehensive investigation of the general distribution

$$X|r, a, b, c \sim f_{X|r,a,b,c}(x) = \int_0^1 f_{X|r,p}^{(\text{NB})}(x) f_{p|a,b,c}^{(\text{GB1})}(p) dp, \quad (4)$$

various special cases are well known. These include:

- (1) $X|r, a, b \sim$ Generalized Waring (r, a, b) , introduced by Irwin (1968), with

$$f_{X|r,a,b}^{(\text{GW})}(x) = \int_0^1 f_{X|r,p}^{(\text{NB})}(x) f_{p|a,b,c=1}^{(\text{GB1})}(p) dp$$

$$= \frac{\mathbf{B}(x+a, b+r)}{\mathbf{B}(a, b) x \mathbf{B}(x, r)};$$

(2) $X|a, b \sim \text{Waring}(a, b) \equiv \text{Generalized Waring}(r=1, a, b)$, with

$$\begin{aligned} f_{X|a,b}^{(W)}(x) &= \int_0^1 f_{X|r=1,p}^{(\text{NB})}(x) f_{p|a,b,c=1}^{(\text{GB1})}(p) dp \\ &= \frac{\mathbf{B}(x+a, b+1)}{\mathbf{B}(a, b)}; \end{aligned} \quad (5)$$

and

(3) $X|b \sim \text{Yule}(b) \equiv \text{Generalized Waring}(r=1, a=1, b)$, with

$$\begin{aligned} f_{X|b}^{(Y)}(x) &= \int_0^1 f_{X|r=1,p}^{(\text{NB})}(x) f_{p|a=1,b,c=1}^{(\text{GB1})}(p) dp \\ &= b \mathbf{B}(x+1, b+1). \end{aligned}$$

To show that $f_{p|a,b,c}^{(\text{GB1})}(p)$ belongs to $\mathcal{M}_{\text{NB}}^{\mathcal{H}}$ (and therefore that $X|r, a, b, c$ of (4) belongs to \mathcal{H}_{D}), we first note that $\lim_{p \rightarrow 1^-} \frac{1-p^c}{1-p} = \lim_{p \rightarrow 1^-} cp^{c-1} = c > 0$ by a straightforward application of L'Hôpital's rule. It then follows from condition (a) of Theorem 1 that

$$\begin{aligned} \lim_{p \rightarrow 1^-} f_{p|a,b,c}^{(\text{GB1})}(p) (1-p)^{-\delta+1} &= \lim_{p \rightarrow 1^-} \frac{c}{\mathbf{B}(a, b)} p^{ca-1} (1-p^c)^{b-1} (1-p)^{-\delta+1} \\ &= \frac{c}{\mathbf{B}(a, b)} \lim_{p \rightarrow 1^-} \left(\frac{1-p^c}{1-p} \right)^{b-1} (1-p)^{b-1} (1-p)^{-\delta+1} \\ &= \frac{c^b}{\mathbf{B}(a, b)} \lim_{p \rightarrow 1^-} (1-p)^{b-\delta}, \end{aligned}$$

which is greater than 0 for all $\delta \geq b$.

Of course, not all PDFs on $(0, 1)$ belong to $\mathcal{M}_{\text{NB}}^{\mathcal{H}}$. An example of a distribution that fails to satisfy the conditions of the above theorem is the Logit-Normal (μ, σ) PDF, $f_{p|\mu,\sigma}^{(\text{LN})}(p) = \frac{1}{\sqrt{2\pi}} \frac{1}{p(1-p)} \exp\left(-\frac{(\text{logit}(p)-\mu)^2}{2\sigma^2}\right)$, for $\mu \in (-\infty, \infty)$ and $\sigma \in (0, \infty)$. In this case,

$$\begin{aligned} \lim_{p \rightarrow 1^-} f_{p|\mu,\sigma}^{(\text{LN})}(p) (1-p)^{-\delta+1} &= \lim_{p \rightarrow 1^-} \frac{1}{\sqrt{2\pi}} \frac{1}{p(1-p)} e^{-\frac{(\text{logit}(p)-\mu)^2}{2\sigma^2}} (1-p)^{-\delta+1} \\ &= \frac{1}{\sqrt{2\pi}} \lim_{p \rightarrow 1^-} \frac{1}{(1-p)^\delta} e^{-\frac{(\text{logit}(p)-\mu)^2}{2\sigma^2}} \end{aligned}$$

$$\begin{aligned}
&= \frac{1}{\sqrt{2\pi}} \lim_{z \rightarrow \infty} \frac{1}{(e^z + 1)^{-\delta}} e^{-\frac{(z-\mu)^2}{2\sigma^2}} \quad (\text{for } z = \text{logit}(p)) \\
&= \frac{1}{\sqrt{2\pi}} \lim_{z \rightarrow \infty} \frac{(e^z + 1)^\delta}{e^{\frac{(z-\mu)^2}{2\sigma^2}}} \\
&= \frac{1}{\sqrt{2\pi}} \lim_{z \rightarrow \infty} \frac{O(e^{\delta z})}{e^{\frac{z^2}{2\sigma^2}} e^{-\frac{z\mu}{\sigma^2}} e^{\frac{\mu^2}{2\sigma^2}}} \\
&= \frac{e^{-\frac{\mu^2}{2\sigma^2}}}{\sqrt{2\pi}} \lim_{z \rightarrow \infty} \frac{O\left(e^{\left(\delta + \frac{\mu}{\sigma^2}\right)z}\right)}{e^{\frac{z^2}{2\sigma^2}}} \\
&= 0
\end{aligned}$$

for all $\delta > 0$.

3.2 Identifiability and Calibrative Families

When using a Negative Binomial mixture model such as (3), it may be desirable to know whether or not the mixed random variable (in this case, $X|r, \boldsymbol{\eta} \sim f_{X|r, \boldsymbol{\eta}}(x)$) can be associated with a unique mixing distribution (i.e., $p|\boldsymbol{\eta} \sim f_{p|\boldsymbol{\eta}}(p)$). This property, known as identifiability, is necessary if one wishes to estimate the parameters of the mixing distribution from observations of the mixed random variable (see, e.g., Xekalaki and Panaretos, 1983). If the r parameter is fixed, then such mixtures are indeed identifiable (see Sapatinas, 1995). However, if r is a random variable, then the mixture

$$X|\boldsymbol{\xi}, \boldsymbol{\eta} \sim f_{X|\boldsymbol{\xi}, \boldsymbol{\eta}}(x) = \int_0^\infty \int_0^1 f_{X|r, p}^{(\text{NB})}(x) f_{r, p|\boldsymbol{\xi}, \boldsymbol{\eta}}(r, p) dp dr,$$

for some joint mixing PDF, $f_{r, p|\boldsymbol{\xi}, \boldsymbol{\eta}}(r, p)$, is generally not identifiable. For example, if there exists a set of unique mixing PDFs, $f_{p|r, \boldsymbol{\eta}}(p)$, such that $f_{X|\boldsymbol{\eta}}(x) = f_{X|r, \boldsymbol{\eta}}(x) = \int_0^1 f_{X|r, p}^{(\text{NB})}(x) f_{p|r, \boldsymbol{\eta}}(p) dp$ is invariant over $r \in \mathcal{I}$, for some interval $\mathcal{I} \subset (0, \infty)$, then $f_{r, p|\boldsymbol{\xi}, \boldsymbol{\eta}}(r, p)$ cannot be unique because it may be expressed as $f_{r, p|\boldsymbol{\xi}, \boldsymbol{\eta}}(r, p) = f_{r|\boldsymbol{\xi}}(r) f_{p|r, \boldsymbol{\eta}}(p)$ for any PDF $f_{r|\boldsymbol{\xi}}(r)$, $r \in \mathcal{I}$.

We will call a set of unique mixing PDFs, $f_{p|r, \boldsymbol{\eta}}(p)$, with invariant $f_{X|\boldsymbol{\eta}}(x) = f_{X|r, \boldsymbol{\eta}}(x) = \int_0^1 f_{X|r, p}^{(\text{NB})}(x) f_{p|r, \boldsymbol{\eta}}(p) dp$ on $r \in \mathcal{I}$, the ‘‘calibrative’’ family for $f_{X|\boldsymbol{\eta}}(x)$ (on $r \in \mathcal{I}$). The following result, which applies to all types of Negative Binomial mixtures (i.e., not just those belonging to \mathcal{H}_D) shows how to construct the calibrative family for a given $f_{X|\boldsymbol{\eta}}(x)$, beginning with only the single member $f_{p|r=1, \boldsymbol{\eta}}(p)$ (corresponding to the Geometric (p) \equiv Negative Binomial ($r = 1, p$) PDF, $f_{X|r=1, p}^{(\text{NB})}(x)$). In practical applications, knowing the form of a calibrative family as a function of r would be useful for testing the fit of

$X|\boldsymbol{\eta} \sim f_{X|\boldsymbol{\eta}}(x) = \int_0^1 f_{X|r,p}^{(\text{NB})}(x) f_{p|r,\boldsymbol{\eta}}(p) dp$ for a known, estimated, or hypothesized value of r .

Theorem 2: For a given loss frequency $X|\boldsymbol{\eta} \sim f_{X|\boldsymbol{\eta}}(x)$, if there exists a PDF, $f_{p|\boldsymbol{\eta}}(p) = f_{p|r=1,\boldsymbol{\eta}}(p)$, satisfying $f_{X|\boldsymbol{\eta}}(x) = \int_0^1 f_{X|r=1,p}^{(\text{NB})}(x) f_{p|\boldsymbol{\eta}}(p) dp$, then:

(1) $f_{p|\boldsymbol{\eta}}(p)$ is unique;

(2) for all $r \in (1, \infty)$, the function

$$f_{p|r>1,\boldsymbol{\eta}}(p) = \frac{(r-1)}{(1-p)^r} \int_p^1 \frac{(\omega-p)^{r-2} (1-\omega)}{\omega^{r-1}} f_{p|\boldsymbol{\eta}}(\omega) d\omega \quad (6)$$

is the unique PDF satisfying $f_{X|\boldsymbol{\eta}}(x) = \int_0^1 f_{X|r>1,p}^{(\text{NB})}(x) f_{p|r>1,\boldsymbol{\eta}}(p) dp$; and

(3) for all $r \in (0, 1)$, the function

$$\begin{aligned} f_{p|r<1,\boldsymbol{\eta}}(p) &= \frac{1}{(1-p)^r} \int_p^1 \frac{(\omega-p)^{r-1}}{\omega^{r-1}} \left[1 + (r-1) \frac{(1-\omega)}{\omega} \right] f_{p|\boldsymbol{\eta}}(\omega) d\omega \\ &\quad - \frac{1}{(1-p)^r} \int_p^1 \frac{(\omega-p)^{r-1} (1-\omega)}{\omega^{r-1}} f'_{p|\boldsymbol{\eta}}(\omega) d\omega \end{aligned} \quad (7)$$

is either the unique PDF or a quasi-PDF (such that $f_{p|r<1,\boldsymbol{\eta}}(p) < 0$ for some $p \in (0, 1)$) satisfying $f_{X|\boldsymbol{\eta}}(x) = \int_0^1 f_{X|r<1,p}^{(\text{NB})}(x) f_{p|r<1,\boldsymbol{\eta}}(p) dp$.

Proof: See Subsection A.2 of the Appendix.

Naturally, the appearance of quasi-PDFs in part (3) of the above theorem is somewhat surprising. The result below, which provides both necessary and sufficient conditions for $f_{p|r<1,\boldsymbol{\eta}}(p) < 0$, shows that quasi-PDFs arise because of the behavior of the original mixing PDF, $f_{p|\boldsymbol{\eta}}(p) = f_{p|r=1,\boldsymbol{\eta}}(p)$, for values of p in a neighborhood of 0. Thus, this issue is not directly related to that of heavy tails, which (as we know from Theorem 1) are associated with the behavior of $f_{p|\boldsymbol{\eta}}(p)$ for values of p close to 1.

Theorem 3: The function $f_{p|r<1,\boldsymbol{\eta}}(p)$ of part (3) of Theorem 2 is characterized by the following two pairs of necessary and sufficient conditions:

(1) $f_{p|r<1,\boldsymbol{\eta}}(p)$ is a quasi-PDF with $f_{p|r<1,\boldsymbol{\eta}}(p) \leq \ell < 0$ in some neighborhood of 0 if

$$(a) \text{ either (i) } \lim_{p \rightarrow 0^+} f_{p|\boldsymbol{\eta}}(p) < \infty \text{ or (ii) } \lim_{p \rightarrow 0^+} f_{p|\boldsymbol{\eta}}(p) = \infty \cap \lim_{p \rightarrow 0^+} \frac{-p f'_{p|\boldsymbol{\eta}}(p)}{f_{p|\boldsymbol{\eta}}(p)} < 1 - r;$$

and only if

$$(b) \text{ either (i) } \lim_{p \rightarrow 0^+} f_{p|\boldsymbol{\eta}}(p) < \infty \text{ or (ii) } \lim_{p \rightarrow 0^+} f_{p|\boldsymbol{\eta}}(p) = \infty \cap \lim_{p \rightarrow 0^+} \frac{-p f'_{p|\boldsymbol{\eta}}(p)}{f_{p|\boldsymbol{\eta}}(p)} \leq 1 - r.$$

(2) $f_{p|r<1,\boldsymbol{\eta}}(p)$ is the unique PDF if

$$(a) \lim_{p \rightarrow 0^+} f_{p|\boldsymbol{\eta}}(p) = \infty \cap \lim_{p \rightarrow 0^+} \frac{-p f'_{p|\boldsymbol{\eta}}(p)}{f_{p|\boldsymbol{\eta}}(p)} \geq 1 - r \cap \frac{-p f'_{p|\boldsymbol{\eta}}(p)}{f_{p|\boldsymbol{\eta}}(p)} > 1 - r - \frac{p}{1-p} \text{ for all } p \in (0, 1),$$

and only if

$$(b) \lim_{p \rightarrow 0^+} f_{p|\eta}(p) = \infty \cap \lim_{p \rightarrow 0^+} \frac{-p f'_{p|\eta}(p)}{f_{p|\eta}(p)} \geq 1 - r.$$

Proof: See Subsection A.3 of the Appendix.

It is worth noting that the sufficient condition provided by (1)(a) of the above theorem can be sharpened by adding constraints on higher-order derivatives of $f_{p|\eta}(p)$ that imply $\lim_{p \rightarrow 0^+} f_{p|r < 1, \eta}(p) < 0$ when $\lim_{p \rightarrow 0^+} f_{p|\eta}(p) = \infty$ and $\lim_{p \rightarrow 0^+} \frac{-p f'_{p|\eta}(p)}{f_{p|\eta}(p)} = 1 - r$. For example, applying L'Hôpital's rule to the indeterminate form of (A5) (of the Appendix) reveals that

$$\lim_{p \rightarrow 0^+} f_{p|\eta}(p) = \infty \cap \lim_{p \rightarrow 0^+} \frac{-p f'_{p|\eta}(p)}{f_{p|\eta}(p)} = 1 - r \cap \lim_{p \rightarrow 0^+} \frac{-p f''_{p|\eta}(p)}{f'_{p|\eta}(p)} < 2 - r$$

also is a sufficient condition for a quasi-PDF with negative values in a neighborhood of 0. However, the usefulness of such incremental improvements is limited because it is relatively easy to find mixing PDFs, $f_{p|\eta}(p)$, that fail to satisfy the enhanced conditions but still yield $\lim_{p \rightarrow 0^+} f_{p|r < 1, \eta}(p) < 0$. A simple example is given by the Kumaraswamy (b, c) PDF with $c = r$,

$$f_{p|b, c=r}^{(K)}(p) = r b p^{r-1} (1 - p^r)^{b-1},$$

for which $\lim_{p \rightarrow 0^+} f_{p|\eta}(p) = \infty$, $\lim_{p \rightarrow 0^+} \frac{-p f'_{p|\eta}(p)}{f_{p|\eta}(p)} = 1 - r$, and $\lim_{p \rightarrow 0^+} \frac{-p f''_{p|\eta}(p)}{f'_{p|\eta}(p)} = 2 - r$, but

$$\begin{aligned} \lim_{p \rightarrow 0^+} f_{p|r < 1, \eta}(p) &= 1 + r^2 b (b - 1) \lim_{p \rightarrow 0^+} \int_p^1 \frac{(1 - \omega)}{(1 - \omega^r) \omega} \omega^{2r-1} (1 - \omega^r)^{b-1} d\omega \\ &= -\infty \end{aligned}$$

for all $r \in (0, 1/2)$ and $b \in (0, 1)$.

3.3 Mixtures of Poisson Counts

It is well known that any Negative Binomial random variable can be expressed as a unique continuous mixture of Poisson random variables. Specifically,

$$f_{X|r, p}^{(NB)}(x) = \int_0^\infty f_{X|\lambda}^{(P)}(x) f_{\lambda|r, \frac{1-p}{p}}^{(\Gamma)}(\lambda) d\lambda, \quad (8)$$

where $f_{X|\lambda}^{(P)}(x) = \frac{e^{-\lambda}\lambda^x}{x!}$, $x \in \{0, 1, 2, \dots\}$ and $f_{\lambda|r, \frac{1-p}{p}}^{(\Gamma)}(\lambda) = \frac{1}{\Gamma(r)} \left(\frac{1-p}{p}\right)^r \lambda^{r-1} \exp\left(-\left(\frac{1-p}{p}\right)\lambda\right)$, $\lambda \in (0, \infty)$ denote the Poisson (λ) PMF and Gamma $\left(r, \frac{1-p}{p}\right)$ PDF, respectively. This fact, in conjunction with Theorem 2, allows one to show that any Negative Binomial mixture $f_{X|\eta}(x) = \int_0^1 f_{X|r,p}^{(NB)}(x) f_{p|\eta}(p) dp$ with calibrative family $f_{p|\eta}(p)$ also can be expressed as a unique Poisson mixture, $f_{X|\eta}(x) = \int_0^\infty f_{X|\lambda}^{(P)}(x) f_{\lambda|\eta}(\lambda) d\lambda$. In practical applications, knowing the form of the PDF $f_{\lambda|\eta}(\lambda)$ would be useful for testing the fit of $X|\eta \sim f_{X|\eta}(x) = \int_0^\infty f_{X|\lambda}^{(P)}(x) f_{\lambda|\eta}(\lambda) d\lambda$.

Theorem 4: For a given loss frequency $X|\eta \sim f_{X|\eta}(x)$, if there exists a PDF, $f_{p|\eta}(p) = f_{p|r=1,\eta}(p)$, satisfying $f_{X|\eta}(x) = \int_0^1 f_{X|r=1,p}^{(NB)}(x) f_{p|\eta}(p) dp$, then the function

$$f_{\lambda|\eta}(\lambda) = \int_0^1 \left(\frac{1-p}{p}\right) \exp\left(-\left(\frac{1-p}{p}\right)\lambda\right) f_{p|\eta}(p) dp$$

is the unique PDF satisfying $f_{X|\eta}(x) = \int_0^\infty f_{X|\lambda}^{(P)}(x) f_{\lambda|\eta}(\lambda) d\lambda$.

Proof: See Subsection A.4 of the Appendix.

4 The ZY(b, c) Distribution

4.1 Definition

We now introduce the discrete two-parameter ‘‘ZY (b, c)’’ distribution, named for the Zeta and Yule families it contains as special cases. Let $X|b, c \sim \text{ZY}(b, c)$ be defined by its PMF,

$$f_{X|b,c}^{(\text{ZY})}(x) = \frac{\text{B}\left(\frac{x+1}{c}, b+1\right)}{\Sigma_{\text{B}}\left(\frac{1}{c}, \frac{1}{c}, b\right)} \quad (9)$$

for $x \in \{0, 1, 2, \dots\}$, with $b \in (0, \infty)$ and $c \in (0, \infty)$, where

$$\Sigma_{\text{B}}(\gamma, u, w) = \sum_{k=0}^{\infty} \text{B}(\gamma k + u, w + 1). \quad (10)$$

Given the relatively complex nature of $\Sigma_{\text{B}}\left(\frac{1}{c}, \frac{1}{c}, b\right)$, it often is easier to work with the PMF ratio, $\frac{f_{X|b,c}^{(\text{ZY})}(x)}{f_{X|b,c}^{(\text{ZY})}(x+1)}$, for arbitrary $x \in \{0, 1, 2, \dots\}$, rather than the PMF itself.

From (9) and (10), it is clear that both $f_{X|b,c}^{(\text{ZY})}(x) \geq 0$ for all $x \in \{0, 1, 2, \dots\}$ and $\sum_{x=0}^{\infty} f_{X|b,c}^{(\text{ZY})}(x) = 1$. Furthermore, the PMF is not only well-behaved for all values of its sample and parameter spaces, but also in

the limit as $c \rightarrow 0^+$.

Taking the relevant limit of the PMF ratio yields

$$\begin{aligned}
\frac{f_{X|b,c=0}^{(ZY)}(x)}{f_{X|b,c=0}^{(ZY)}(x+1)} &= \lim_{c \rightarrow 0^+} \frac{\Gamma\left(\frac{x+1}{c}\right) \Gamma\left(\frac{x+2}{c} + b + 1\right)}{\Gamma\left(\frac{x+1}{c} + b + 1\right) \Gamma\left(\frac{x+2}{c}\right)} \\
&= \lim_{\tau \rightarrow \infty} \frac{\Gamma(\tau(x+1)) \Gamma(\tau(x+2) + b + 1)}{\Gamma(\tau(x+1) + b + 1) \Gamma(\tau(x+2))} \\
&= \lim_{\tau \rightarrow \infty} \frac{\sqrt{\frac{2\pi}{\tau(x+1)}} \left(\frac{\tau(x+1)}{e}\right)^{\tau(x+1)} \sqrt{\frac{2\pi}{\tau(x+2) + b + 1}} \left(\frac{\tau(x+2) + b + 1}{e}\right)^{\tau(x+2) + b + 1}}{\sqrt{\frac{2\pi}{\tau(x+1) + b + 1}} \left(\frac{\tau(x+1) + b + 1}{e}\right)^{\tau(x+1) + b + 1} \sqrt{\frac{2\pi}{\tau(x+2)}} \left(\frac{\tau(x+2)}{e}\right)^{\tau(x+2)}}, \quad (11)
\end{aligned}$$

where (11) is obtained by replacing all gamma functions with Stirling's approximation. This expression then simplifies to

$$\begin{aligned}
&\lim_{\tau \rightarrow \infty} \sqrt{\frac{\tau(x+2)}{\tau(x+1)}} \sqrt{\frac{\tau(x+1) + b + 1}{\tau(x+2) + b + 1}} \left(\frac{\tau(x+1)}{\tau(x+1) + b + 1}\right)^{\tau(x+1)} \\
&\quad \times \left(\frac{\tau(x+2) + b + 1}{\tau(x+2)}\right)^{\tau(x+2)} \left(\frac{\tau(x+2) + b + 1}{\tau(x+1) + b + 1}\right)^{b+1} \\
&= \lim_{\tau \rightarrow \infty} \sqrt{\frac{\tau(x+2)}{\tau(x+1)}} \sqrt{\frac{\tau(x+1) + b + 1}{\tau(x+2) + b + 1}} \left(1 - \frac{b+1}{\tau(x+1) + b + 1}\right)^{\tau(x+1) + b + 1} \\
&\quad \times \left(1 + \frac{b+1}{\tau(x+2)}\right)^{\tau(x+2)} \left(\frac{\tau(x+2) + b + 1}{\tau(x+1)}\right)^{b+1} \\
&= \sqrt{\frac{x+2}{x+1}} \sqrt{\frac{x+1}{x+2}} e^{-(b+1)} e^{b+1} \left(\frac{x+2}{x+1}\right)^{b+1} \\
&= \left(\frac{x+2}{x+1}\right)^{b+1},
\end{aligned}$$

which is the corresponding PMF ratio from (1) for $s = b + 1$. Thus, we will say that $X|b \sim \text{Zeta}(b + 1)$ constitutes a special case of $X|b, c \sim \text{ZY}(b, c)$ as $c \rightarrow 0^+$.

Setting $c = 1$ in (9) yields a more immediate result:

$$\frac{f_{X|b,c=1}^{(ZY)}(x)}{f_{X|b,c=1}^{(ZY)}(x+1)} = \frac{\Gamma(x+1) \Gamma(x+b+3)}{\Gamma(x+b+2) \Gamma(x+2)},$$

which is the indicated PMF ratio from (2). Consequently, we also can conclude that $X|b \sim \text{Yule}(b)$ forms a

special case of $X|b, c \sim ZY(b, c)$ for $c = 1$.

4.2 Mixtures of Negative Binomial and Poisson Counts

It is instructive to show that $X|b, c \sim ZY(b, c)$ – and therefore $X|b \sim \text{Zeta}(b + 1)$ and $X|b \sim \text{Yule}(b)$ – can be formed as unique, continuous mixtures of both Negative Binomial and Poisson random variables. This is accomplished by first finding a PDF, $f_{p|b,c}(p)$, such that $f_{X|b,c}^{(ZY)}(x) = \int_0^1 f_{X|r=1,p}^{(NB)}(x) f_{p|b,c}(p) dp$, and then applying the results of Theorems 2 and 4 to identify $f_{p|r,b,c}(p)$ and $f_{\lambda|b,c}(p)$, respectively.

Part (A) of the following result provides what we will call the “Sigma-B (b, c)” mixing distribution, $f_{p|b,c}^{(\Sigma_B)}(p) \sim \Sigma_B(b, c)$, for $c \in (0, \infty)$, and part (B) addresses the limiting case of $c \rightarrow 0^+$.

Theorem 5:

(A) For $X|b, c > 0 \sim ZY(b, c > 0)$, the function

$$f_{p|b,c>0}^{(\Sigma_B)}(p) = \frac{c}{\Sigma_B\left(\frac{1}{c}, \frac{1}{c}, b\right)} \frac{(1-p)^b}{(1-p)^c}, \quad (12)$$

with $\Sigma_B\left(\frac{1}{c}, \frac{1}{c}, b\right)$ as defined in (17), is the unique PDF satisfying $f_{X|b,c>0}^{(ZY)}(x) = \int_0^1 f_{X|r=1,p}^{(NB)}(x) f_{p|b,c>0}^{(\Sigma_B)}(p) dp$.

(B) For $X|b, c \rightarrow 0 \sim ZY(b, c \rightarrow 0)$, the function

$$f_{p|b,c\rightarrow 0}^{(\Sigma_B)}(p) = \frac{(-\ln(p))^b}{\zeta(b+1) \Gamma(b+1) (1-p)} \quad (13)$$

is the unique PDF satisfying $f_{X|b,c\rightarrow 0}^{(ZY)}(x) = \int_0^1 f_{X|r=1,p}^{(NB)}(x) f_{p|b,c\rightarrow 0}^{(\Sigma_B)}(p) dp$.

Proof: See Subsection A.5 of the Appendix.

The next result, addressing Negative Binomial mixtures, follows directly from Theorem 2. Again, part (A) considers the case of $c \in (0, \infty)$, and part (B) the limiting case of $c \rightarrow 0^+$.

Corollary 1:

(A) If $X|b, c > 0 \sim ZY(b, c > 0)$, then:

(1) for all $r \in (1, \infty)$, the function

$$f_{p|r>1,b,c>0}(p) = \frac{c(r-1)}{\Sigma_B\left(\frac{1}{c}, \frac{1}{c}, b\right) (1-p)^r} \int_p^1 \frac{(\omega-p)^{r-2} (1-\omega^c)^b}{\omega^{r-1}} d\omega$$

is the unique PDF satisfying $f_{X|b,c>0}^{(ZY)}(x) = \int_0^1 f_{X|r>1,p}^{(NB)}(x) f_{p|r>1,b,c>0}(p) dp$; and

(2) for all $r \in (0, 1)$, the function

$$f_{p|r<1,b,c>0}(p) = \frac{c}{\Sigma_{\mathbf{B}}\left(\frac{1}{c}, \frac{1}{c}, b\right) (1-p)^r} \\ \times \left[bc \int_p^1 \frac{(\omega-p)^{r-1} (1-\omega^c)^{b-1}}{\omega^{r-c}} d\omega + (r-1) \int_p^1 \frac{(\omega-p)^{r-1} (1-\omega^c)^b}{\omega^r} d\omega \right]$$

is a quasi-PDF satisfying $f_{X|b,c>0}^{(ZY)}(x) = \int_0^1 f_{X|r<1,p}^{(\text{NB})}(x) f_{p|r<1,b,c>0}(p) dp$, with $f_{p|r<1,b,c>0}(p) \leq \ell < 0$ for all p in some neighborhood of 0.

(B) If $X|b, c \rightarrow 0 \sim ZY(b, c \rightarrow 0)$, then:

(1) for all $r \in (1, \infty)$, the function

$$f_{p|r>1,b,c\rightarrow 0}(p) = \frac{(r-1)}{\zeta(b+1) \Gamma(b+1) (1-p)^r} \int_p^1 \frac{(\omega-p)^{r-2} (-\ln(\omega))^b}{\omega^{r-1}} d\omega$$

is the unique PDF satisfying $f_{X|b,c\rightarrow 0}^{(ZY)}(x) = \int_0^1 f_{X|r>1,p}^{(\text{NB})}(x) f_{p|r>1,b,c\rightarrow 0}(p) dp$; and

(2) for all $r \in (0, 1)$, the function

$$f_{p|r<1,b,c\rightarrow 0}(p) = \frac{1}{\zeta(b+1) \Gamma(b+1) (1-p)^r} \\ \times \left[b \int_p^1 \frac{(\omega-p)^{r-1} (-\ln(\omega))^{b-1}}{\omega^r} d\omega + (r-1) \int_p^1 \frac{(\omega-p)^{r-1} (-\ln(\omega))^b}{\omega^r} d\omega \right]$$

is a quasi-PDF satisfying $f_{X|b,c\rightarrow 0}^{(ZY)}(x) = \int_0^1 f_{X|r<1,p}^{(\text{NB})}(x) f_{p|r<1,b,c\rightarrow 0}(p) dp$, with $f_{p|r<1,b,c\rightarrow 0}(p) \leq \ell < 0$ for all p in some neighborhood of 0.

Proof: See Subsection A.6 of the Appendix.

The intuition behind $f_{p|r<1,b,c>0}(p) < 0$ and $f_{p|r<1,b,c\rightarrow 0}(p) < 0$ in certain neighborhoods of 0 is fairly straightforward. Essentially, when $r \in (0, 1)$, the Negative Binomial PMF becomes very steep for values of x close to (and including) 0 (e.g., $\sup_r \left(\frac{f_{X|r,p}^{(\text{NB})}(0)}{f_{X|r,p}^{(\text{NB})}(1)} \right) = \lim_{r \rightarrow 0^+} \frac{1}{r^p} = \infty$), and this steepness is aggravated for values of p close to zero. Consequently, for small values of x , it is impossible to construct the much flatter ZY PMF (for which both $\inf_b \left(\frac{f_{X|b,c>0}^{(ZY)}(0)}{f_{X|b,c>0}^{(ZY)}(1)} \right) = \lim_{b \rightarrow 0^+} \frac{\Gamma(\frac{1}{c}) \Gamma(\frac{2}{c} + b + 1)}{\Gamma(\frac{1}{c} + b + 1) \Gamma(\frac{2}{c})} = 2$ and $\inf_b \left(\frac{f_{X|b,c\rightarrow 0}^{(ZY)}(0)}{f_{X|b,c\rightarrow 0}^{(ZY)}(1)} \right) = \lim_{b \rightarrow 0^+} 2^{b+1} = 2$) as a convex combination of Negative Binomial PMFs. However, if one can assign negative weight to those Negative Binomial PMFs for which p is very small, then the impact of small r can be mitigated by offsetting it with negative contributions from small p .

Although we previously showed that $X|b, c \sim \text{ZY}(b, c)$ is heavy-tailed for both $c \rightarrow 0^+$ and $c = 1$ (by virtue of the fact that both the Zeta and Yule distributions, respectively, are heavy-tailed), a direct proof that $\text{ZY}(b, c) \in \mathcal{H}_D$ for all $c > 0$ was not readily apparent. However, given that $X|b, c > 0 \sim \text{ZY}(b, c > 0)$ can be constructed as mixtures of Negative Binomial ($r = 1, p$) random variables by part (A) of Theorem 5, it now is possible to demonstrate the heavy-tailed nature of all ZY random variables for $c > 0$ by applying Theorem 1. From our earlier analysis of the Generalized Beta 1 distribution, we know that $\lim_{p \rightarrow 1^-} \frac{1-p^c}{1-p} = \lim_{p \rightarrow 1^-} cp^{c-1} = c > 0$ by L'Hôpital's rule. It then follows that

$$\begin{aligned} \lim_{p \rightarrow 1^-} f_{p|b, c > 0}(p) (1-p)^{-\delta+1} &= \lim_{p \rightarrow 1^-} \frac{c}{\Sigma_B\left(\frac{1}{c}, \frac{1}{c}, b\right)} \frac{(1-p^c)^b}{(1-p)} (1-p)^{-\delta+1} \\ &= \frac{c}{\Sigma_B\left(\frac{1}{c}, \frac{1}{c}, b\right)} \lim_{p \rightarrow 1^-} \left(\frac{1-p^c}{1-p}\right)^b (1-p)^{b-\delta} \\ &= \frac{c^{b+1}}{\Sigma_B\left(\frac{1}{c}, \frac{1}{c}, b\right)} \lim_{p \rightarrow 1^-} (1-p)^{b-\delta}, \end{aligned}$$

which is greater than 0 for all $\delta \geq b$.

We turn to Poisson mixtures in the next result, which follows directly from Theorem 4. As in Theorem 5 and Corollary 1, part (A) considers the case of $c \in (0, \infty)$, and part (B) the limiting case of $c \rightarrow 0^+$.

Corollary 2:

(A) If $X|b, c > 0 \sim \text{ZY}(b, c > 0)$, then the function

$$f_{\lambda|b, c > 0}(\lambda) = \frac{c}{\Sigma_B\left(\frac{1}{c}, \frac{1}{c}, b\right)} \int_0^\infty \frac{1}{y+1} \left[1 - \left(\frac{1}{y+1}\right)^c\right]^b \exp(-\lambda y) dy \quad (14)$$

is the unique PDF satisfying $f_{X|b, c > 0}^{(\text{ZY})}(x) = \int_0^\infty f_{X|\lambda}^{(\text{P})}(x) f_{\lambda|b, c > 0}(\lambda) d\lambda$.

(B) If $X|b, c \rightarrow 0 \sim \text{ZY}(b, c \rightarrow 0)$, then the function

$$f_{\lambda|b, c \rightarrow 0}(\lambda) = \frac{1}{\zeta(b+1) \Gamma(b+1)} \int_0^\infty \frac{1}{y+1} (\ln(y+1))^b \exp(-\lambda y) dy \quad (15)$$

is the unique PDF satisfying $f_{X|b, c \rightarrow 0}^{(\text{ZY})}(x) = \int_0^\infty f_{X|\lambda}^{(\text{P})}(x) f_{\lambda|b, c \rightarrow 0}(\lambda) d\lambda$.

Proof: See Subsection A.7 of the Appendix.

4.3 Comparison with the Waring(a, b) Distribution

The PMF of the two-parameter ZY distribution, (9), offers a range of functional shapes similar to those of the two-parameter Waring distribution, (5), and both are reasonably versatile choices for modeling heavy-tailed loss frequencies. In fact, the two distributions' tail behaviors are nearly identical, with tail parameter b playing essentially the same role in both cases. However, for values of x close to (and including) 0, the ZY and Waring PMFs are more distinct, with the former tending to assume flatter shapes than the latter for any fixed value of b (e.g., $\frac{f_{X|b,c}^{(ZY)}(0)}{f_{X|b,c}^{(ZY)}(1)} \in (1, 2^{b+1})$, whereas $\frac{f_{X|a,b}^{(W)}(0)}{f_{X|a,b}^{(W)}(1)} \in (1, \infty)$). As a consequence, the Waring distribution does not include the Zeta model as a special case (although it does include the Yule model when $a = 1$, as noted in Subsection 3.1). Another notable difference is that the the ZY PMF is more complex than the Waring PMF (because of the former's normalization constant), and therefore likely to require more complex statistical-estimation procedures. On the other hand, the ZY distribution allows one to differentiate between the Zeta and Yule models through hypothesis tests based on the estimated value of the c parameter.

The next result, addressing Negative Binomial mixtures, follows from Theorem 2.

Corollary 3:

If $X|a, b \sim \text{Waring}(a, b)$, then:

(1) for all $r \in (1, \infty)$, the function

$$f_{p|r>1,a,b}(p) = \frac{(r-1)}{\mathbf{B}(a,b)(1-p)^r} \int_p^1 \frac{(\omega-p)^{r-2} (1-\omega)^b}{\omega^{r-a}} d\omega$$

is the unique PDF satisfying $f_{X|a,b}^{(W)}(x) = \int_0^1 f_{X|r>1,p}^{(NB)}(x) f_{p|r>1,a,b}(p) dp$; and

(2) for all $r \in (0, 1)$ such that $r \geq a$, the function

$$f_{p|r<1,a,b}(p) = \frac{1}{\mathbf{B}(a,b)(1-p)^r} \\ \times \left[(r-a) \int_p^1 \frac{(\omega-p)^{r-1} (1-\omega)^{b-1}}{\omega^{r-a+1}} d\omega - (r-a-b) \int_p^1 \frac{(\omega-p)^{r-1} (1-\omega)^{b-1}}{\omega^{r-a}} d\omega \right]$$

is the unique PDF satisfying $f_{X|a,b}^{(W)}(x) = \int_0^1 f_{X|r<1,p}^{(NB)}(x) f_{p|r<1,a,b}(p) dp$; and

(3) for all $r \in (0, 1)$ such that $r < a$, the function in part (2) above is a quasi-PDF satisfying $f_{X|a,b}^{(W)}(x) = \int_0^1 f_{X|r<1,p}^{(NB)}(x) f_{p|r<1,a,b}(p) dp$, with $f_{p|r<1,a,b}(p) \leq \ell < 0$ for all p in some neighborhood of 0.

Proof: See Subsection A.8 of the Appendix.

The next result, addressing Poisson mixtures, follows from Theorem 4.

Corollary 4:

If $X|a, b > 0 \sim \text{Waring}(a, b)$, then the function

$$f_{\lambda|a,b}(\lambda) = \frac{1}{\mathbf{B}(a, b)} \int_0^\infty \frac{y^b}{(y+1)^{a+b}} \exp(-y\lambda) dy \quad (16)$$

is the unique PDF satisfying $f_{X|a,b}^{(\text{W})}(x) = \int_0^\infty f_{X|\lambda}^{(\text{P})}(x) f_{\lambda|a,b}(\lambda) d\lambda$.

Proof: See Subsection A.9 of the Appendix.

5 Extensions and Unification

Comparing the analytical forms of the heavy-tailed ZY (b, c) and Waring (a, b) PMFs is rather difficult because the index (x) appears as an argument of beta functions in both cases. Alternatively, it is quite easy to compare the associated mixing distributions that give rise to these families as mixtures of a Negative Binomial $(r = 1, p)$ random variable; that is, the Sigma-B (b, c) and Beta (a, b) PDFs, respectively. Recognizing that

$$f_{p|b,c}^{(\Sigma_B)}(p) = \frac{c}{\Sigma_B\left(\frac{1}{c}, \frac{1}{c}, b\right)} \frac{(1-p^c)^b}{(1-p)} \propto \frac{(1-p^c)^b}{(1-p)}$$

and

$$f_{p|a,b}^{(\text{B})}(p) = \frac{1}{\mathbf{B}(a, b)} p^{a-1} (1-p)^{b-1} \propto p^{a-1} (1-p)^{b-1},$$

one can see that introducing a third parameter into each PDF can bring their functional forms closer together in a natural way. In particular, $f_{p|b,c}^{(\Sigma_B)}(p)$ can be extended to what we will call the ‘‘Generalized Sigma-B (a, b, c) ’’ PDF,

$$f_{p|a,b,c}^{(\text{G}\Sigma_B)}(p) = \frac{c}{\Sigma_B\left(\frac{1}{c}, a, b\right)} \frac{p^{ca-1} (1-p^c)^b}{(1-p)} \propto \frac{p^{ca-1} (1-p^c)^b}{(1-p)}, \quad (17)$$

by inserting a factor of p^{ca-1} ; whereas $f_{p|a,b}^{(\text{B})}(p)$ can be extended to the Generalized Beta 1 (a, b, c) PDF,

$$f_{p|a,b,c}^{(\text{GB1})}(p) = \frac{c}{\mathbf{B}(a, b)} p^{ca-1} (1-p^c)^{b-1} \propto p^{ca-1} (1-p^c)^{b-1}, \quad (18)$$

by transforming p to p^c .

Using (17) and (18) to construct mixtures of Negative Binomial $(r = 1, p)$ random variables then yields

the following heavy-tailed generalizations of the ZY and Waring distributions, respectively:

$$f_{X|a,b,c}^{(\text{GZY})}(x) = \frac{\Sigma_{\mathbf{B}}\left(\frac{1}{c}, \frac{x}{c} + a, b\right) - \Sigma_{\mathbf{B}}\left(\frac{1}{c}, \frac{(x+1)}{c} + a, b\right)}{\Sigma_{\mathbf{B}}\left(\frac{1}{c}, a, b\right)}, \quad (19)$$

to be called the ‘‘Generalized ZY (a, b, c) ’’ distribution; and

$$f_{X|a,b,c}^{(\text{GW2})}(x) = \frac{\mathbf{B}\left(\frac{x}{c} + a, b\right) - \mathbf{B}\left(\frac{(x+1)}{c} + a, b\right)}{\mathbf{B}(a, b)}, \quad (20)$$

to be called the ‘‘Generalized Waring 2 (a, b, c) ’’ distribution (to distinguish it from the three-parameter Generalized Waring distribution mentioned in Subsection 3.1). Obviously, the above two PMFs are quite similar, with each of the three infinite series of (19) truncated to its first term in (20).

To unify (19) and (20) into a single, four-parameter PMF, we again turn to the associated mixing PDFs (in (17) and (18), respectively), and note that these two cases are easily assumed into what we will call the ‘‘Hyper-Generalized Sigma-B (a, b, c, d) ’’ PDF,

$$f_{p|a,b,c,d}^{(\text{HG}\Sigma_{\mathbf{B}})}(p) = \frac{c}{\Sigma_{\mathbf{B}}\left(\frac{d}{c}, a, b\right)} \frac{p^{ca-1} (1-p^c)^b}{(1-p^d)}, \quad (21)$$

by introducing the parameter $d \in (0, \infty)$ as an exponent of p in the denominator. Using (21) to form a Negative Binomial ($r = 1, p$) mixture then extends the Generalized ZY and Generalized Waring 2 distributions to the heavy-tailed model

$$f_{X|a,b,c,d}^{(\text{HGZY})}(x) = \frac{\Sigma_{\mathbf{B}}\left(\frac{d}{c}, \frac{x}{c} + a, b\right) - \Sigma_{\mathbf{B}}\left(\frac{d}{c}, \frac{(x+1)}{c} + a, b\right)}{\Sigma_{\mathbf{B}}\left(\frac{d}{c}, a, b\right)},$$

to be called the ‘‘Hyper-Generalized ZY (a, b, c, d) ’’ distribution.

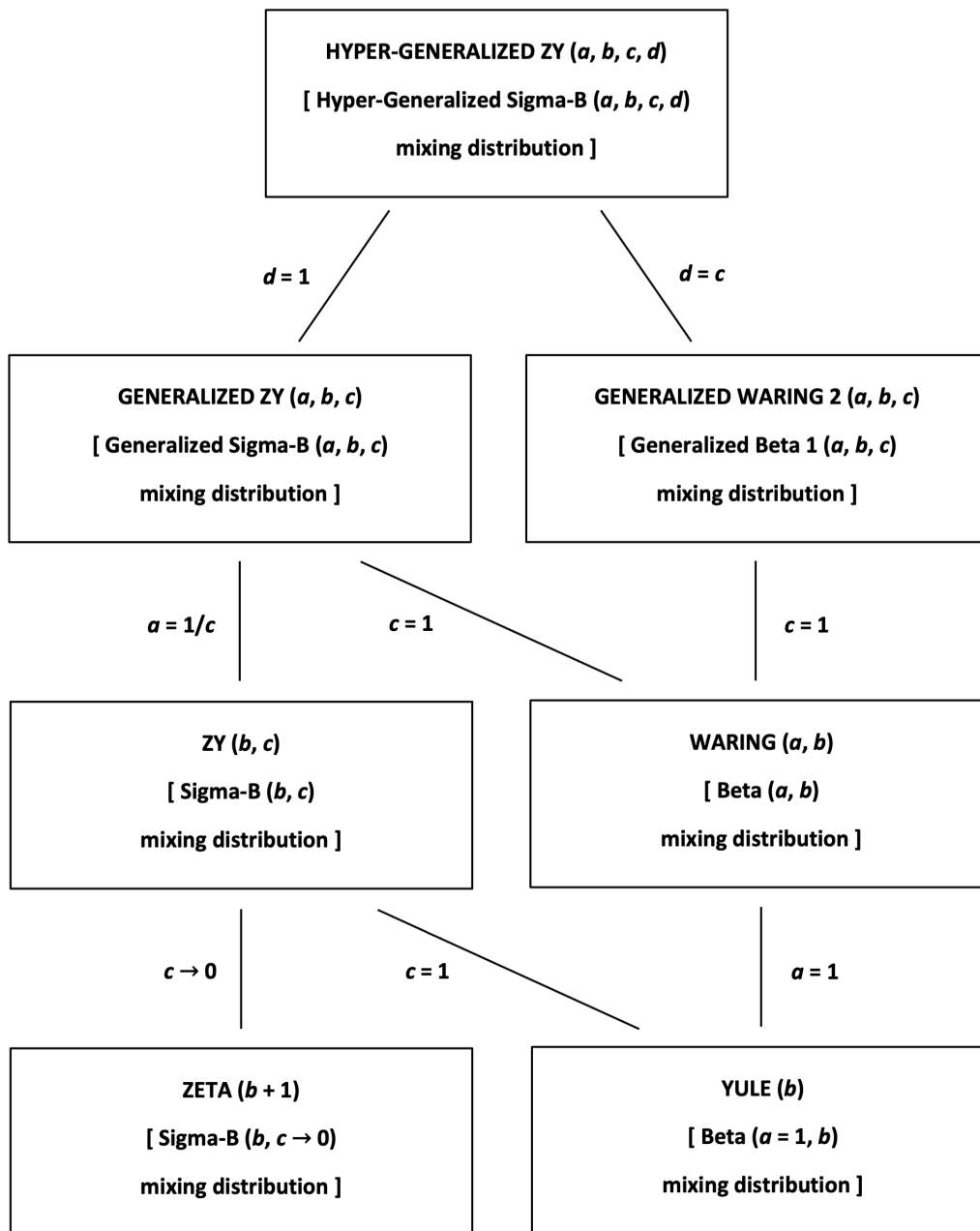


Figure 1. Hierarchy of Distributions within the Hyper-Generalized ZY Family

Figure 1 summarizes the parametric hierarchy among members of the heavy-tailed Hyper-Generalized ZY family, which we will denote by \mathcal{HG} . Although these relationships may be of theoretical interest to some researchers, our purpose in formulating the \mathcal{HG} family of discrete distributions – together with the corresponding family of continuous mixing distributions – is more pragmatic. Basically, we wish to provide a

new and useful approach to analyzing empirical loss frequencies in concert with conventional GLM methods. Specifically, we would note that, after modeling frequency data with a flexible (and possibly multi-parameter) probability distribution, one can decompose the fitted distribution into either a Negative Binomial or Poisson mixture via the formulas of Theorems 2 and 4, respectively.⁴ This approach is conceptually consistent with conventional GLM regression, in which loss frequencies are modeled as aggregates of either Negative Binomial or Poisson components associated with individual risk classifications, and the exposure-weighted means of the various risk classifications form an implicit mixing distribution. Comparing the GLM mixing distribution with the theoretical mixing distribution of Theorem 2 or 4 thus affords a direct means of testing the robustness of GLM methods.

6 Application to Historical Loss Data

In this section, the modeling approach described in Section 5 is applied to a classic set of Swedish commercial motor-vehicle insurance loss data first studied by Hallin and Ingenbleek (1983). Since the purpose of our analysis is primarily illustrative – that is, to demonstrate the usefulness of multiple-parameter loss-frequency models based on mixtures of Poisson and Negative Binomial counts – we do not provide a comprehensive investigation of the data. Consequently, certain statistical issues, such as potential collinearity among the explanatory variables, correlation between loss frequency and loss severity, and the presence of outliers, will not be considered.

The relevant data set is introduced in Subsection 6.1. We then carry out the following three procedures (in Subsections 6.2-6.4, respectively):

(1) fitting the various one- to four-parameter members of \mathcal{HG} to the aggregate loss-frequency counts by maximum likelihood;

(2) fitting the aggregate loss-frequency data by Poisson and Negative Binomial GLM regression to estimate the mixing distributions implied by the exposure-weighted means of the various risk classifications; and

(3) fitting the distributions of parameter estimates generated by the Poisson and Negative Binomial GLM regressions by the theoretical mixing distributions associated with the members of \mathcal{HG} .

⁴In the Negative Binomial case, this can be done for various fixed values of the r parameter.

6.1 Swedish Commercial Motor-Vehicle Data

Sweden’s 1977 portfolio of commercial motor-vehicle third-party insurance loss data was introduced to the actuarial literature by Hallin and Ingenbleek (1983) for purposes of investigating a new methodology for risk-based pricing. These data then were included in a compilation of data sets by Andrews and Herzberg (1985), and subsequently used by numerous researchers (see, e.g.: Smyth and Jørgensen, 2002; Frees, 2010; Pigeon and Denuit, 2011; Pan, Soo, and Pooi, 2014; Dunn and Smyth, 2018; and Zhang, 2021). One important characteristic of the Swedish commercial motor-vehicle portfolio is the heavy tail of its empirical loss-frequency distribution, which appears not to have been discussed in prior articles.

The Swedish data are broken down by policyholder and motor-vehicle characteristics, with 2182 sub-portfolios (line items) in total. Each line item, $i = 1, 2, \dots, 2182$, includes seven fields:

- (a) number of kilometers driven (as one of 5 ranges: $[0, 1000)$, $[1000, 15,000)$, $[15,000, 20,000)$, $[20,000, 25,000)$, $[25,000, \infty)$);
- (b) geographical zone (as one of 7 regions⁵);
- (c) no-claim bonus status ($= \min \{1 + \text{number of years since last claim}, 7\}$);
- (d) motor-vehicle make (as one of 9 categories: 8 specific models plus 1 “all other”);
- (e) number of exposures (insured-vehicle policy years), E_i ;
- (f) number of loss events (recorded as claims), X_i ; and
- (g) total losses (in Swedish Krona);

and is formed by a unique combination of risk classifications (items (a)-(d)) aggregated over all insurance companies.

Summary statistics from the empirical distribution of the X_i are presented in Table 1, and include notably large coefficients of skewness and kurtosis. The high degree of positive skewness is clear from the plot of the empirical histogram in Figure 2, and the heavy right tail confirmed by the plot of the empirical hazard function in Figure 3, which tends to 0 for large values in the sample space.

Table 1. Summary Statistics of Swedish Motor-Vehicle Frequencies, X_i

No. of Obs.	Minimum	Maximum	Mean	Std. Dev.	Skewness	Kurtosis
2182	0	3338	51.87	201.71	8.57	96.36

⁵See Hallin and Ingenbleek (1983) for descriptions of the geographical zones and motor-vehicle makes.

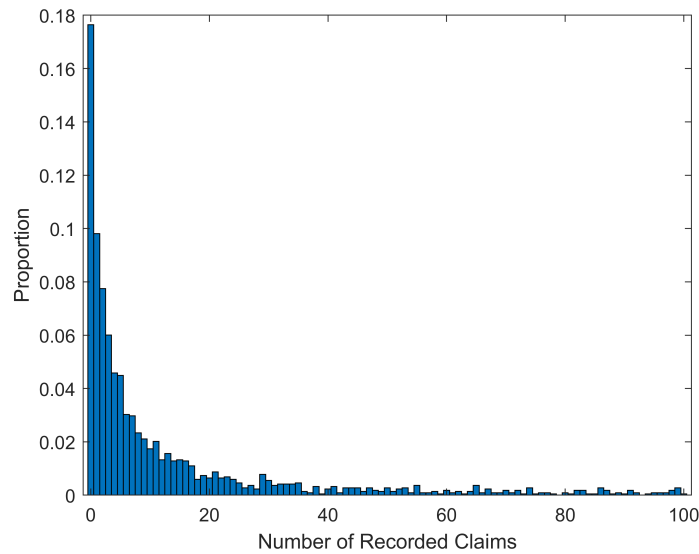


Figure 2. Swedish Motor-Vehicle Frequencies, Empirical Histogram

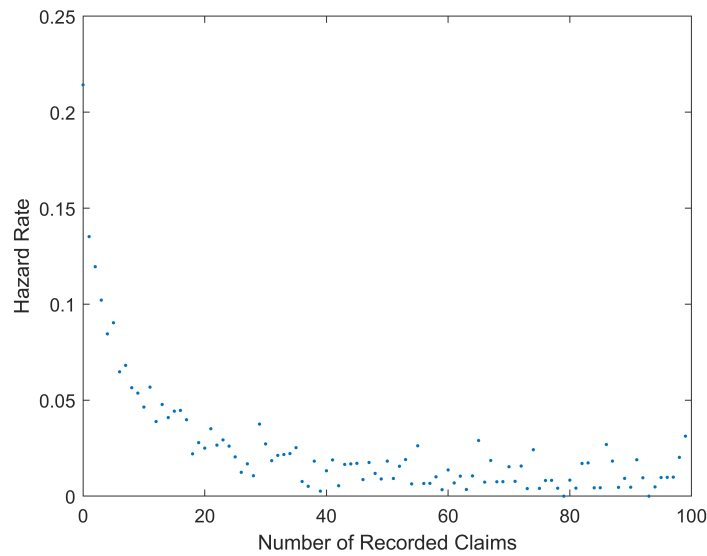


Figure 3. Swedish Motor-Vehicle Frequencies, Empirical Hazard Function

The observed tail characteristics suggest that the frequency data may be well modeled by one or more members of \mathcal{HG} . However, it is important to note that much of the tail behavior is explained by heavy tails in the empirical distribution of exposures. This is shown in Table 2, Figures 4, and Figure 5, which demonstrate skewness and heavy-tail properties comparable to those of the empirical frequency distribution. In the context of the present analysis, this means that: (1) when fitting a member of \mathcal{HG} to the data, it is likely that the underlying exposure characteristics strongly influence the relevant mixing distribution; and (2) in applying GLM regression, the exposures constitute a natural offset.

Table 2. Summary Statistics of Swedish Motor-Vehicle Exposures, E_i

No. of Obs.	Minimum	Maximum	Mean	Std. Dev.	Skewness	Kurtosis
2182	0.01	127,687.27	1092.20	5661.16	13.96	253.49

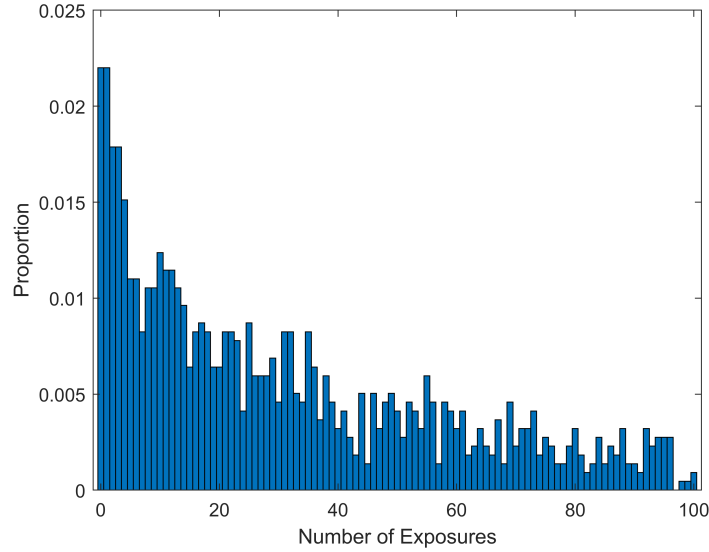


Figure 4. Swedish Motor-Vehicle Exposures, Empirical Histogram

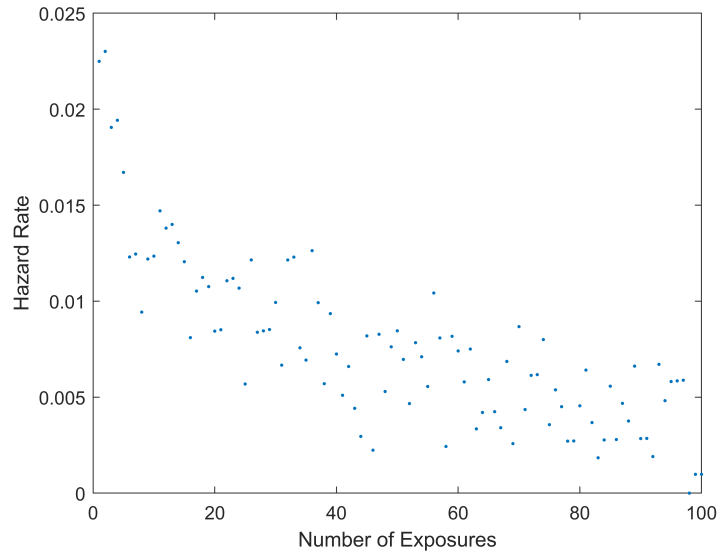


Figure 5. Swedish Motor-Vehicle Exposures, Empirical Hazard Function

6.2 Fitting \mathcal{HG} Frequency Models

We fit the seven members of \mathcal{HG} to the motor-vehicle frequencies, X_i , using the method of maximum likelihood. As shown in Table 3, this provides useful results in all but one case – that of the three-parameter

GW2 (a, b, c) distribution – for which the likelihood function possesses no interior maximum.

Table 3. Maximum-Likelihood Estimation of \mathcal{HG} Parameters

Distribution	\hat{a}	\hat{b}	\hat{c}	\hat{d}	Log(Likelihood)
HGZY (a, b, c, d)	0.0049 (0.0040)*	3.3112 (2.8519)	939.1870 (809.2498)	70.0691 (23.8098)	-8668.78
GZY (a, b, c)	0.0727 (0.0290)	0.8997 (0.0670)	23.6117 (6.9803)		-8675.28
GW2 (a, b, c)	---	---	---		<i>Fails to converge</i>
ZY (b, c)		1.0909 (0.0919)	60.8621 (10.1789)		-8690.72
Waring (a, b)	3.9178 (0.2755)	0.7431 (0.0287)			-8682.03
Zeta ($b + 1$)		0.3733 (0.0086)			-8927.62
Yule (b)		0.4138 (0.0100)			-8876.67

* Estimated standard errors of parameter estimators are shown in parentheses.

To assess which (if any) of the \mathcal{HG} distributions fit the motor-vehicle data well, we first employ the maximum-likelihood parameter estimates to compute minimum- χ^2 statistics for each of the feasible six members. Table 4 shows that, at commonly used levels of significance, the minimum- χ^2 test rejects the null hypothesis (that the motor-vehicle frequency data come from the indicated distribution) for the ZY (b, c), Zeta ($b + 1$), and Yule (b) models. To compare the relative suitability of the remaining three distributions, we next consider the Akaike information criterion (AIC) and Bayesian information criterion (BIC), provided in the two rightmost columns of the same table. Both of these measures suggest that, even after including explicit penalties for additional parameters, the four-parameter HGZY (a, b, c, d) is preferred to the three-parameter GZY (a, b, c), which in turn is preferred to the two-parameter Waring (a, b).

Table 4. Goodness-of-Fit Measures for \mathcal{HG} Distributions

Distribution	Min.- χ^2 Statistic	Degrees of Freedom	p -Value	AIC	BIC
HGZY (a, b, c, d)	24.57	$29^* - 4 - 1 = 24$	0.4291	17,345.56	17,368.32
GZY (a, b, c)	26.88	$32 - 3 - 1 = 28$	0.5246	17,356.56	17,373.62
ZY (b, c)	64.65	$31 - 2 - 1 = 28$	0.0001		
Waring (a, b)	27.71	$30 - 2 - 1 = 27$	0.4260	17,368.06	17,379.44
Zeta ($b + 1$)	327.88	$22 - 1 - 1 = 20$	< 0.0001		
Yule (b)	273.67	$23 - 1 - 1 = 21$	< 0.0001		

* In computing the minimum- χ^2 statistic for a given distribution, the cells consist of all nonnegative integers x such that $2182 \times \Pr \{X = x\} \geq 10$, plus 1 additional cell for all remaining integers x .

6.3 Applying GLM Regression

Distributional modeling of portfolio loss frequencies, such as that performed in the previous subsection, offers no direct information about the loss propensities of individual risk classifications. For this reason, actuaries typically work with GLM or similar regression methods that permit the estimation of each risk classification’s contribution to overall losses. Although a wide array of sophisticated extensions and generalizations of GLM regression are now available (see, e.g., Goldburd, Khare, Tevet, and Guller, 2020), the basic GLM framework for expected loss-frequency with Poisson and/or Negative Binomial observations remains an integral part of actuarial practice. Therefore, we illustrate the usefulness of our mixing-distribution approach by fitting the Swedish motor-vehicle data with a simple GLM with natural-log link function and exposures as offset,

$$\ln(\mu_i) = \ln(E_i) + \beta_0 + \mathbf{Y}_i^{(\text{KILO})} \boldsymbol{\beta}^{(\text{KILO})} + \mathbf{Y}_i^{(\text{ZONE})} \boldsymbol{\beta}^{(\text{ZONE})} + \mathbf{Y}_i^{(\text{BONUS})} \boldsymbol{\beta}^{(\text{BONUS})} + \mathbf{Y}_i^{(\text{MAKE})} \boldsymbol{\beta}^{(\text{MAKE})}, \quad (22)$$

where:

$\mathbf{Y}_i^{(\text{KILO})}$, $\mathbf{Y}_i^{(\text{ZONE})}$, $\mathbf{Y}_i^{(\text{BONUS})}$, and $\mathbf{Y}_i^{(\text{MAKE})}$ denote line item i ’s four fields (from (a)-(d) from Subsection 6.1) encoded as matrices of indicator variables;

$$\mu_i = E \left[X_i \mid E_i, \mathbf{Y}_i^{(\text{KILO})}, \mathbf{Y}_i^{(\text{ZONE})}, \mathbf{Y}_i^{(\text{BONUS})}, \mathbf{Y}_i^{(\text{MAKE})} \right]; \text{ and either}$$

$$\text{(I) } X_i \mid E_i, \mathbf{Y}_i^{(\text{KILO})}, \mathbf{Y}_i^{(\text{ZONE})}, \mathbf{Y}_i^{(\text{BONUS})}, \mathbf{Y}_i^{(\text{MAKE})} \sim \text{independent Poisson } (\lambda_i) \text{ or}$$

$$\text{(II) } X_i \mid E_i, \mathbf{Y}_i^{(\text{KILO})}, \mathbf{Y}_i^{(\text{ZONE})}, \mathbf{Y}_i^{(\text{BONUS})}, \mathbf{Y}_i^{(\text{MAKE})} \sim \text{independent Negative Binomial } (r, p_i).$$

For simplicity, the formulation with Poisson observations will be called “Model I”, and that with Negative Binomial observations “Model II”.

From (22), it is clear that both Models I and II include the full set of four risk-classification variables described in Subsection 6.1. For completeness, we ran GLM regressions using all subsets of these four

variables, and found that both the AIC and BIC were minimized under the full model for both the Poisson and Negative Binomial cases. Therefore, only the full-model results are presented in Tables 5 and 6.

Table 5. Model I (Poisson) Regression Results

Log(Likelihood)	Residual-Deviance χ^2 Statistic	Degrees of Freedom	p-Value
-5302.00	2966.12	2182 - 25 = 2157	< 0.0001
Parameter	Estimate	Standard Error	z-Value
β_0	-1.8128	0.0138	-131.7754
$\beta_2^{(KILO)}$	0.2126	0.0075	28.2549
$\beta_3^{(KILO)}$	0.3202	0.0087	36.9737
$\beta_4^{(KILO)}$	0.4047	0.0121	33.5715
$\beta_5^{(KILO)}$	0.5760	0.0128	44.8916
$\beta_2^{(ZONE)}$	-0.2382	0.0095	-25.0820
$\beta_3^{(ZONE)}$	-0.3864	0.0097	-39.9587
$\beta_4^{(ZONE)}$	-0.5819	0.0087	-67.2428
$\beta_5^{(ZONE)}$	-0.3261	0.0145	-22.4455
$\beta_6^{(ZONE)}$	-0.5262	0.0119	-44.3086
$\beta_7^{(ZONE)}$	-0.7310	0.0407	-17.9617
$\beta_2^{(BONUS)}$	-0.4790	0.0121	-39.6069
$\beta_3^{(BONUS)}$	-0.6932	0.0135	-51.3160
$\beta_4^{(BONUS)}$	-0.8274	0.0146	-56.7348
$\beta_5^{(BONUS)}$	-0.9256	0.0140	-66.2689
$\beta_6^{(BONUS)}$	-0.9935	0.0116	-85.4294
$\beta_7^{(BONUS)}$	-1.3274	0.0087	-152.8445
$\beta_2^{(MAKE)}$	0.0762	0.0212	3.5898
$\beta_3^{(MAKE)}$	-0.2474	0.0251	-9.8594
$\beta_4^{(MAKE)}$	-0.6535	0.0242	-27.0218
$\beta_5^{(MAKE)}$	0.1549	0.0202	7.6564
$\beta_6^{(MAKE)}$	-0.3356	0.0174	-19.3139
$\beta_7^{(MAKE)}$	-0.0559	0.0233	-2.3965
$\beta_8^{(MAKE)}$	-0.0439	0.0316	-1.3901
$\beta_9^{(MAKE)}$	-0.0681	0.0100	-6.8356

Table 6. Model II (Negative Binomial) Regression Results

Log(Likelihood)	Residual-Deviance χ^2 Statistic	Degrees of Freedom	<i>p</i> -Value
-5163.80	2229.91	2182 - 26 = 2156	0.1307
Parameter	Estimate	Standard Error	<i>z</i> -Value
<i>r</i>	110.5986	14.8104	7.4676
β_0	-1.7822	0.0238	-75.0413
$\beta_2^{(KILO)}$	0.1885	0.0150	12.5337
$\beta_3^{(KILO)}$	0.2753	0.0162	17.0058
$\beta_4^{(KILO)}$	0.3521	0.0193	18.2378
$\beta_5^{(KILO)}$	0.5167	0.0201	25.7438
$\beta_2^{(ZONE)}$	-0.2242	0.0179	-12.5241
$\beta_3^{(ZONE)}$	-0.3828	0.0181	-21.2094
$\beta_4^{(ZONE)}$	-0.5559	0.0170	-32.7396
$\beta_5^{(ZONE)}$	-0.3386	0.0225	-15.0191
$\beta_6^{(ZONE)}$	-0.5225	0.0200	-26.1238
$\beta_7^{(ZONE)}$	-0.7307	0.0462	-15.8003
$\beta_2^{(BONUS)}$	-0.4428	0.0214	-20.7266
$\beta_3^{(BONUS)}$	-0.6805	0.0224	-30.3736
$\beta_4^{(BONUS)}$	-0.8204	0.0231	-35.4871
$\beta_5^{(BONUS)}$	-0.9191	0.0224	-41.0399
$\beta_6^{(BONUS)}$	-0.9931	0.0203	-48.8821
$\beta_7^{(BONUS)}$	-1.3259	0.0177	-74.8806
$\beta_2^{(MAKE)}$	0.0673	0.0256	2.6263
$\beta_3^{(MAKE)}$	-0.2352	0.0294	-7.9859
$\beta_4^{(MAKE)}$	-0.6836	0.0293	-23.3053
$\beta_5^{(MAKE)}$	0.1523	0.0245	6.2119
$\beta_6^{(MAKE)}$	-0.3633	0.0221	-16.4340
$\beta_7^{(MAKE)}$	-0.0791	0.0277	-2.8564
$\beta_8^{(MAKE)}$	-0.0411	0.0352	-1.1695
$\beta_9^{(MAKE)}$	-0.0903	0.0157	-5.7576

The contents of these two tables show that Model II affords a better fit to the motor-vehicle data than Model I. This is most apparent from comparing the respective *p*-values, since Model I's value (< 0.0001) strongly supports rejecting (22) with the Poisson assumption, whereas Model II's value (0.1307) does not support rejecting (22) with the Negative Binomial assumption at common levels of significance. Furthermore, a close inspection of the *z*-values associated with the individual risk classifications reveals these quantities to be substantially more variable in Model I than Model II, suggesting that the former model gives disproportionate leverage to risk classifications with less overdispersion.

In the next subsection, we will use these models to analyze the mixing distributions implied by the exposure-weighted means of the various risk classifications, providing insights into the relationship between the mixing distributions and overall model fit. For both Models I and II, the set of exposure-weighted risk-classification means is given by

$$\hat{\mu}_i = E_i \exp \left(\beta_0 + \mathbf{Y}_i^{(\text{KILO})} \hat{\beta}^{(\text{KILO})} + \mathbf{Y}_i^{(\text{ZONE})} \hat{\beta}^{(\text{ZONE})} + \mathbf{Y}_i^{(\text{BONUS})} \hat{\beta}^{(\text{BONUS})} + \mathbf{Y}_i^{(\text{MAKE})} \hat{\beta}^{(\text{MAKE})} \right),$$

for $i = 1, 2, \dots, 2182$. In Model I, these estimates immediately generate an implied “sample” of the Poisson parameter, λ , by setting $\hat{\lambda}_i = \hat{\mu}_i$. In Model II, they generate an analogous “sample” of the Negative Binomial parameter, p , by taking $\hat{p}_i = \frac{\hat{\mu}_i}{\hat{\mu}_i + \hat{r}}$. Histograms of the $\hat{\lambda}_i$ and \hat{p}_i are presented in Figures 6 and 7, respectively.

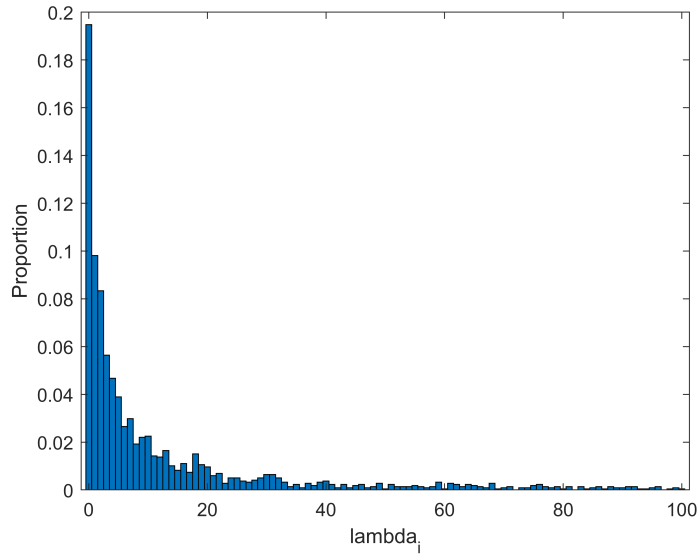


Figure 6. Histogram of Estimated λ_i from Model I

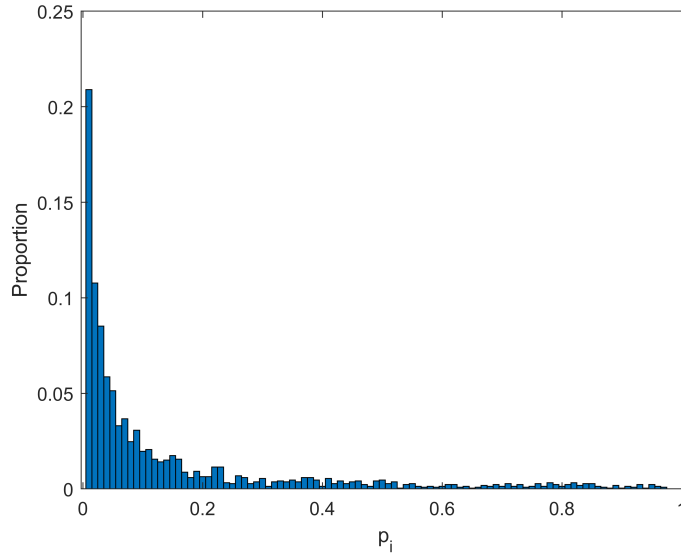


Figure 7. Histogram of Estimated p_i from Model II

6.4 Testing Theoretical Mixing Distributions

Theorem 4 of Subsection 3.3 allows one to calculate the mixing PDFs for the Poisson parameter λ associated with the HGZY (a, b, c, d) , GZY (a, b, c) , and Waring (a, b) distributions. These theoretical distributions then may be fit to the $\hat{\lambda}_i$ of Model I, yielding the results presented in Tables 7 and 8. Since Model I does not provide a good overall fit to the Swedish motor-vehicle data, we would not expect the theoretical mixing distributions to fit the $\hat{\lambda}_i$ very well; and that is indeed the case. Table 8 shows that the minimum- χ^2 test rejects the null hypothesis (that the $\hat{\lambda}_i$ come from the indicated mixing distribution) at the 0.05 significance level for all three PDFs.

Table 7. Maximum-Likelihood Estimation of λ Mixing-Distribution Parameters (Model I)

Distribution	\hat{a}	\hat{b}	\hat{c}	\hat{d}	Log(Likelihood)
$f_{\lambda a,b,c,d}(\lambda)$ for HGZY (a, b, c, d)	0.0060 (0.0049)*	2.7456 (1.9963)	740.1885 (640.6377)	60.5348 (22.4654)	-8529.05
$f_{\lambda a,b,c}(\lambda)$ for GZY (a, b, c)	0.0650 (0.0195)	0.9156 (0.0636)	25.6792 (6.0218)		-8525.61
$f_{\lambda a,b}(\lambda)$ for Waring (a, b)	3.7199 (0.2443)	0.7252 (0.0272)			-8540.27

* Estimated standard errors of parameter estimators are shown in parentheses.

Table 8. Goodness-of-Fit Measures for λ Mixing Distributions (Model I)

Distribution	Min.- χ^2 Statistic	Degrees of Freedom	p -Value	AIC	BIC
$f_{\lambda a,b,c,d}(\lambda)$ for HGZY (a, b, c, d)	44.14	$28^* - 4 - 1 = 23$	0.0051	17,066.09	17,088.85
$f_{\lambda a,b,c}(\lambda)$ for GZY (a, b, c)	41.69	$31 - 3 - 1 = 27$	0.0353	17,057.23	17,074.29
$f_{\lambda a,b}(\lambda)$ for Waring (a, b)	40.72	$29 - 2 - 1 = 26$	0.0331	17,084.54	17,095.91

* In computing the minimum- χ^2 statistic for a given mixing distribution, the cells consist of all intervals $(n, n + 1]$, where n is a nonnegative integer such that $2182 \times \Pr\{\lambda \in (n, n + 1]\} \geq 10$, plus 1 additional cell for all remaining integers n .

Theorem 2(2) of Subsection 3.2 permits the calculation of mixing PDFs for the Negative Binomial parameter p , given the (fixed) estimated value of r , $\hat{r} = 110.5986$, for the same three members of the \mathcal{HG} family. Fitting these theoretical distributions to the p_i of Model II yields the results summarized in Tables 9 and 10. Since Model II provides a reasonable overall fit to the motor-vehicle data, it is not surprising that the theoretical mixing distributions also fit the \hat{p}_i fairly well. In fact, Table 8 shows that the minimum- χ^2 test does not reject the null hypothesis (that the \hat{p}_i come from the indicated mixing distribution) at the 0.05 level for the PDFs associated with the GZY (a, b, c) and Waring (a, b) distributions.

Table 9. Maximum-Likelihood Estimation of p Mixing-Distribution Parameters (Model II)

Distribution	\hat{a}	\hat{b}	\hat{c}	\hat{d}	Log(Likelihood)
$f_{p a,b,c,d}(p)$ for HGZY (a, b, c, d)	0.0073 (0.0062)*	2.3350 (1.4930)	592.7998 (533.7293)	54.0534 (22.7704)	2659.55
$f_{p a,b,c}(p)$ for GZY (a, b, c)	0.0620 (0.0183)	0.9187 (0.0641)	26.3941 (6.0980)		2664.30
$f_{p a,b}(p)$ for Waring (a, b)	3.6690 (0.2407)	0.7215 (0.0270)			2648.56

* Estimated standard errors of parameter estimators are shown in parentheses.

Table 10. Goodness-of-Fit Measures for p Mixing Distributions (Model II)

Distribution	Min.- χ^2 Statistic	Degrees of Freedom	p -Value	AIC	BIC
$f_{p a,b,c,d}(p)$ for HGZY (a, b, c, d)	39.80	$28^* - 4 - 1 = 23$	0.0162	-5311.09	-5288.34
$f_{p a,b,c}(p)$ for GZY (a, b, c)	36.34	$31 - 3 - 1 = 27$	0.1081	-5322.60	-5305.54
$f_{p a,b}(p)$ for Waring (a, b)	36.16	$29 - 2 - 1 = 26$	0.0887	-5293.13	-5281.75

* In computing the minimum- χ^2 statistic for a given mixing distribution, the cells consist of all intervals $\left(\frac{n}{n+\hat{r}}, \frac{n+1}{n+1+\hat{r}}\right]$, where n is a nonnegative integer such that $2182 \times \Pr\left\{p \in \left(\frac{n}{n+\hat{r}}, \frac{n+1}{n+1+\hat{r}}\right]\right\} \geq 10$, plus 1 additional cell for all remaining integers n .

The foregoing procedures demonstrate that an analysis of mixing distributions can offer a useful means of validating conclusions based on GLM regression. Although confirming the superiority of Model II to Model I may seem somewhat redundant given the dispositive test results of Tables 5 and 6, it is important to keep in mind that model-selection decisions are not always so clear-cut. This is especially true if one is choosing from among numerous alternative models employing different sets of risk classifications and other covariates.

Additionally, it should be noted that the analysis of mixing distributions also can serve as an effective diagnostic tool. In the case at hand, we see that the preferred model for fitting the motor-vehicle frequency distribution is HGZY (a, b, c, d), whereas the preferred model for fitting the \hat{p}_i of Model II is the mixing distribution associated with GZY (a, b, c). This tells us that the GLM regression with Negative Binomial observations discounts the impact of the \mathcal{HG} family's d parameter, which plays a crucial role in governing the tail behavior of the frequency distribution. Since increasing d over the interval $[1, \infty)$ reduces the heaviness of the frequency tail, Model II effectively overstates the impact of this tail. Although there are many potential explanations for this deviation (e.g., collinearity among the explanatory variables or the presence of statistical outliers), it is likely that the assumption of a fixed Negative Binomial r parameter plays a major role. By applying exploratory GLM regressions to various subsets of the motor-vehicle data, one can see that the r parameter is likely heterogeneous, requiring further modeling.

7 Conclusions

In the present article, we have investigated the class of heavy-tailed frequency models formed by continuous mixtures of Negative Binomial and Poisson random variables. We began by defining the concept of a

calibrative family of mixing distributions, each member of which is identifiable from its associated Negative Binomial mixture, and showed how to construct such families from only a single member. We then introduced the heavy-tailed two-parameter ZY distribution as a generalization of both the one-parameter Zeta and Yule distributions, constructing calibrative families for both the new distribution and the heavy-tailed two-parameter Waring distribution. Finally, we extended both the ZY and Waring families to the four-parameter Hyper-Generalized ZY family, which may be employed in conjunction with the concept of calibrative families to analyze empirical loss-frequency data.

From both theoretical and applied perspectives, it is clear that the assumption of a fixed Negative Binomial r parameter is quite restrictive. Given the general unavailability of calibrative families of joint mixing distributions (of p and r simultaneously; see Subsection 3.2), we believe further research should focus on practical methods for partitioning data into separate components within which the r parameter is relatively homogeneous, while retaining the potential benefits of analyzing mixing distributions.

As indicated at the outset, we hope that the present (and subsequent) work encourages greater interest in the application of heavy-tailed frequency models. However, we also would note that the study of calibrative mixing distributions is equally useful for modeling continuous data, such as loss severities. In the continuous case, the Gamma (r, λ) distribution would constitute the natural analogue of the Negative Binomial (r, p) distribution, with the Exponential (λ) \equiv Gamma ($r = 1, \lambda$) distribution taking over the central role of the Geometric (p) \equiv Negative Binomial ($r = 1, p$) distribution in constructing calibrative families.

References

- [1] Andrews, D. and Herzberg, A., 1985, *Data: A Collection of Problems from Many Fields for the Student and Research Worker*, Springer Verlag, New York, NY, USA.
- [2] Dai, J., Huang, Z., Powers, M. R., and Xu, 2021, “Characterizing the Zeta Distribution via Continuous Mixtures”, arXiv:2008.06200.
- [3] Doray, L. G. and Luong, A., 1995, “Quadratic Distance Estimators for the Zeta Family”, *Insurance: Mathematics and Economics*, 16, 3, 255-260.
- [4] Dunn, P. K. and Smyth, G. K., 2018, *Generalized Linear Models with Examples in R*, Springer Nature, New York, NY, USA.
- [5] Frees, E. W., 2010, *Regression Modeling with Actuarial and Financial Applications*, Cambridge University Press, Cambridge, UK.
- [6] Goldburd, M., Khare, A., Tevet, D., and Guller, D., 2020, *Generalized Linear Models for Insurance Rating*, Second Edition, Casualty Actuarial Society, Arlington, VA, USA.

- [7] Hallin, M. and Ingenbleek, J.-F., 1983, “The Swedish Automobile Portfolio in 1977 – A Statistical Study”, *Scandinavian Actuarial Journal*, 1, 49-64.
- [8] Irwin, J. O., 1968, “The Generalized Waring Distribution Applied to Accident Theory”, *Journal of the Royal Statistical Society: Series A*, 131, 205-207.
- [9] Karlis, D., 2005, “EM Algorithm for Mixed Poisson and Other Discrete Distributions”, *ASTIN Bulletin*, 35, 1, 3-24.
- [10] McDonald, J. B., 1984, “Some Generalized Functions for the Size Distribution of Income”, *Econometrica*, 52, 3, 647-665.
- [11] Newman, M. E. J., 2005, “Power Laws, Pareto Distributions, and Zipf’s Law”, *Contemporary Physics*, 46, 5, 323-351.
- [12] Pan, W. Y., Soo, H. C., and Pooi, A. H., 2014, “Determination of Motor Insurance Rates”, *Proceedings of the International Conference on Mathematics, Statistics, and Financial Mathematics*, Kuala Lumpur, Malaysia.
- [13] Pigeon, M. and Denuit, M., 2011, “Composite Lognormal-Pareto Model with Random Threshold”, *Scandinavian Actuarial Journal*, 2011, 3, 177-192.
- [14] Sapatinas, T., 1995, Identifiability of Mixtures of Power-Series Distributions and Related Characterizations”, *Annals of the Institute of Statistical Mathematics*, 47, 447–459.
- [15] Smyth, G. K. and Jørgensen, B., 2002, “Fitting Tweedie’s Compound Poisson Model to Insurance Claims Data: Dispersion Modelling”, *ASTIN Bulletin*, 32, 1, 143-157.
- [16] Xekalaki, E. and Panaretos, J., 1983, “Identifiability of Compound Poisson Distributions”, *Scandinavian Actuarial Journal*, 66, 39-45.
- [17] Zhang, Z., 2021, “Data Sets Modeling and Frequency Prediction via Machine Learning and Neural Network”, IEEE International Conference on Emergency Science and Information Technology, Chongqing, China.

Appendix

A.1 Proof of Theorem 1

Although $E_{X|r,p}^{(\text{NB})} [X^\delta]$ does not possess a convenient analytic form, it is possible to show, by successive differentiation of the moment-generating function, $\varphi_{X|r,p}^{(\text{NB})} (z) = \left(\frac{1-p}{1-pz}\right)^r$, that

$$(1-p)^r \sum_{i=1}^{\delta} \frac{\Gamma(r+1)}{\Gamma(r+1-i)} [S_0(z)]^{r-i} [S_1(z)]^i \leq \frac{\partial^\delta}{\partial z^\delta} \varphi_{X|r,p}^{(\text{NB})} (z) \leq (1-p)^r \sum_{i=1}^{\delta} \frac{\Gamma(r+1)}{\Gamma(r+1-i)} [S_0(z)]^{r-i} [S_\delta(z)]^i$$

for all $\delta \in \{1, 2, 3, \dots\}$ and $z \geq 0$, where $S_0(z) = \frac{1}{1-pe^z} = 1 + \sum_{j=1}^{\infty} (pe^z)^j$ and $S_k(z) = \frac{\partial^k}{\partial z^k} S_0(z) = \sum_{j=1}^{\infty} j^k (pe^z)^j$ for $k \in \{1, 2, 3, \dots\}$. Taking limits of the above inequalities as $z \rightarrow 0^+$ then yields

$$\begin{aligned} & (1-p)^r \sum_{i=1}^{\delta} \frac{\Gamma(r+1)}{\Gamma(r+1-i)} \left(1 + \sum_{j=1}^{\infty} p^j\right)^{r-i} \left(\sum_{j=1}^{\infty} j p^j\right)^i \leq E_{X|r,p}^{(\text{NB})} [X^\delta] \\ & \leq (1-p)^r \sum_{i=1}^{\delta} \frac{\Gamma(r+1)}{\Gamma(r+1-i)} \left(1 + \sum_{j=1}^{\infty} p^j\right)^{r-i} \left(\sum_{j=1}^{\infty} j^\delta p^j\right)^i \\ \Leftrightarrow & \sum_{i=1}^{\delta} \frac{\Gamma(r+1)}{\Gamma(r+1-i)} \left[\frac{(1-p)pA_1(p)}{(1-p)^2}\right]^i \leq E_{X|r,p}^{(\text{NB})} [X^\delta] \leq \sum_{i=1}^{\delta} \frac{\Gamma(r+1)}{\Gamma(r+1-i)} \left[\frac{(1-p)pA_\delta(p)}{(1-p)^{\delta+1}}\right]^i \\ \Leftrightarrow & \sum_{i=1}^{\delta} \frac{\Gamma(r+1)p^i}{\Gamma(r+1-i)(1-p)^i} \leq E_{X|r,p}^{(\text{NB})} [X^\delta] \leq \sum_{i=1}^{\delta} \frac{\Gamma(r+1)p^i (A_\delta(p))^i}{\Gamma(r+1-i)(1-p)^{\delta i}}, \end{aligned}$$

where $A_k(p)$ denotes the k^{th} -degree Eulerian polynomial (which is of order p^{k-1}). This implies that, for all $\delta \in \{1, 2, 3, \dots\}$ and $r \in (0, \infty)$,

$$Q_1(r, p) \leq E_{X|r,p}^{(\text{NB})} [X^\delta] \leq Q_2(r, p),$$

where both $Q_1(r, p)$ and $Q_2(r, p)$ are increasing functions of p on $(0, 1)$, with $Q_1(r, 0) = Q_2(r, 0) = 0$, $Q_1(r, p) = O\left((1-p)^{-\delta}\right)$, and $Q_2(r, p) = O\left((1-p)^{-\delta^2}\right)$ as $p \rightarrow 1^-$. These properties hold for all $\delta \in (0, \infty)$ by continuity.

We now note that $f_{p|\eta}(p) \in \mathcal{M}_{\text{NB}}^H$ if and only if $E_{X|r,\eta} [X^\delta] = \lim_{n \rightarrow \infty} \sum_{x=0}^n x^\delta f_{X|r,\eta}(x) = \infty$ for some $\delta \in (0, \infty)$. This divergence is equivalent to

$$\int_0^1 E_{X|r,p}^{(\text{NB})} [X^\delta] f_{p|\eta}(p) dp = \infty,$$

which implies

$$\int_0^1 Q_2(r, p) f_{p|\eta}(p) dp = \infty$$

and is implied by

$$\int_0^1 Q_1(r, p) f_{p|\eta}(p) dp = \infty$$

for all $r \in (0, \infty)$.

From statement (b), we know that, for some $\delta \in (0, \infty)$ and any $\varepsilon \in (0, L)$, there exists $p_\varepsilon \in (0, 1)$ such that $p > p_\varepsilon \implies f_{p|\eta}(p) (1-p)^{-\delta+1} \geq L - \varepsilon > 0$. Thus,

$$\lim_{t \rightarrow 1^-} \int_0^t Q_1(r, p) f_{p|\eta}(p) dp \geq \int_0^{p_\varepsilon} Q_1(r, p) f_{p|\eta}(p) dp + \lim_{t \rightarrow 1^-} \int_{p_\varepsilon}^t \frac{Q_1(r, p)}{(1-p)^{-\delta}} \frac{(L - \varepsilon)}{(1-p)} dp,$$

where the second term on the right-hand side equals infinity, implying $\lim_{t \rightarrow 1^-} \int_0^t Q_1(r, p) f_{p|\eta}(p) dp = \infty$ as well. To show that condition (b) is implied by $\lim_{t \rightarrow 1^-} \int_0^t Q_2(r, p) f_{p|\eta}(p) dp = \infty$ for some $\delta \in (0, \infty)$, assume the negation of (b) (i.e., $\lim_{p \rightarrow 1^-} f_{p|\eta}(p) (1-p)^{-\delta+1} = 0$ for all $\delta \in (0, \infty)$, which implies $\lim_{p \rightarrow 1^-} f_{p|\eta}(p) (1-p)^{-\delta^2+1/2} = 0$ for all $\delta \in (0, \infty)$). This means that, for all $\delta \in (0, \infty)$ and any $\varepsilon > 0$, there exists $p_\varepsilon \in (0, 1)$ such that $p > p_\varepsilon \implies f_{p|\eta}(p) (1-p)^{-\delta^2+1/2} \leq \varepsilon$, and so

$$\lim_{t \rightarrow 1^-} \int_0^t Q_2(r, p) f_{p|\eta}(p) dp \leq \int_0^{p_\varepsilon} Q_2(r, p) f_{p|\eta}(p) dp + \lim_{t \rightarrow 1^-} \int_{p_\varepsilon}^t \frac{Q_2(r, p)}{(1-p)^{-\delta^2}} \frac{\varepsilon}{(1-p)^{1/2}} dp,$$

where both terms on the right-hand side are finite, implying the negation of $\lim_{t \rightarrow 1^-} \int_0^t Q_2(r, p) f_{p|\eta}(p) dp = \infty$ for some $\delta \in (0, \infty)$.

To demonstrate the equivalence of statements (b) and (c), first let $R(p) = \frac{\ln(f_{p|\eta}(p))}{\ln(1-p)}$ and rewrite (b) as

$$\lim_{p \rightarrow 1^-} (1-p)^{R(p)-\delta+1} > 0 \text{ for some } \delta \in (0, \infty).$$

Then

$$\lim_{p \rightarrow 1^-} (R(p) - \delta + 1) \ln(1-p) > -\infty \text{ for some } \delta \in (0, \infty)$$

$$\iff \lim_{p \rightarrow 1^-} R(p) \leq \delta - 1 \text{ for some } \delta \in (0, \infty)$$

$$\iff \lim_{p \rightarrow 1^-} \frac{\ln(f_{p|\eta}(p))}{\ln(1-p)} < \infty. \blacksquare$$

A.2 Proof of Theorem 2

For part (1), the uniqueness of $f_{p|\eta}(p)$ follows immediately from the identifiability of Negative Binomial mixtures with fixed r (see Theorem 2.1 of Sapatinas, 1995). For parts (2) and (3), we first derive the expression in (7), which holds for all $r \in (0, \infty)$, and then show that (7) simplifies to (6) for $r \in (1, \infty)$.⁶

⁶The expressions in parts (2) and (3) may be obtained by “brute force” as solutions to Fredholm equations of the first type. However, we have found that a few fortuitous rearrangements (see, e.g., equations (A1) and (A2)) avoid the need for such methods.

First, note that $\int_0^1 f_{X|r,p}^{(\text{NB})}(x) f_{p|r,\eta}(p) dp = f_{X|\eta}(x)$ implies

$$\int_0^1 \frac{\Gamma(x+r)}{\Gamma(r)\Gamma(x+1)} (1-p)^r p^x f_{p|r,\eta}(p) dp = \int_0^1 (1-\omega) \omega^x f_{p|\eta}(\omega) d\omega,$$

or equivalently,

$$\begin{aligned} \int_0^1 (1-p)^r p^x f_{p|r,\eta}(p) dp &= \frac{\Gamma(r)\Gamma(x+1)}{\Gamma(x+r)} \int_0^1 (1-\omega) \omega^x f_{p|\eta}(\omega) d\omega \\ &= \frac{\Gamma(r)\Gamma(x+1)}{\Gamma(x+r)} \left[\frac{(x+1)}{(x+r)} \int_0^1 (1-\omega) \omega^x f_{p|\eta}(\omega) d\omega + \frac{(r-1)}{(x+r)} \int_0^1 (1-\omega) \omega^x f_{p|\eta}(\omega) d\omega \right] \\ &= \mathbf{B}(x+1, r) \left[\int_0^1 \omega^{x+1} f_{p|\eta}(\omega) d\omega + (x+1) \int_0^1 \omega^x f_{p|\eta}(\omega) d\omega \right. \\ &\quad \left. - (x+2) \int_0^1 \omega^{x+1} f_{p|\eta}(\omega) d\omega + (r-1) \int_0^1 (1-\omega) \omega^x f_{p|\eta}(\omega) d\omega \right] \end{aligned} \quad (\text{A1})$$

$$= \mathbf{B}(x+1, r) \left[\int_0^1 \omega^{x+1} f_{p|\eta}(\omega) d\omega - \int_0^1 (1-\omega) \omega^{x+1} f'_{p|\eta}(\omega) d\omega + (r-1) \int_0^1 (1-\omega) \omega^x f_{p|\eta}(\omega) d\omega \right] \quad (\text{A2})$$

(where the middle integral in (A2) results from applying integration by parts to each of the two middle integrals in (A1)). Since $\mathbf{B}(x+1, r) = \int_0^1 t^x (1-t)^{r-1} dt$, it follows that

$$\begin{aligned} \int_0^1 (1-p)^r p^x f_{p|r,\eta}(\omega) d\omega &= \int_0^1 t^x (1-t)^{r-1} dt \left[\int_0^1 \omega^{x+1} f_{p|\eta}(\omega) d\omega \right. \\ &\quad \left. - \int_0^1 (1-\omega) \omega^{x+1} f'_{p|\eta}(\omega) d\omega + (r-1) \int_0^1 (1-\omega) \omega^x f_{p|\eta}(\omega) d\omega \right] \\ &= \int_0^1 \int_0^1 (t\omega)^x (1-t)^{r-1} \omega f_{p|\eta}(\omega) dt d\omega - \int_0^1 \int_0^1 (t\omega)^x (1-t)^{r-1} \omega (1-\omega) f'_{p|\eta}(\omega) dt d\omega \\ &\quad + (r-1) \int_0^1 \int_0^1 (t\omega)^x (1-t)^{r-1} (1-\omega) f_{p|\eta}(\omega) dt d\omega. \end{aligned} \quad (\text{A3})$$

Substituting $p = \omega t$ into all three integrals of (A3) then yields

$$\begin{aligned} \int_0^1 (1-p)^r p^x f_{p|r,\eta}(p) dp &= \int_0^1 \int_0^\omega p^x \left(1 - \frac{p}{\omega}\right)^{r-1} f_{p|\eta}(\omega) dp d\omega \\ &- \int_0^1 \int_0^\omega p^x \left(1 - \frac{p}{\omega}\right)^{r-1} (1-\omega) f'_{p|\eta}(\omega) dp d\omega + (r-1) \int_0^1 \int_0^\omega p^x \left(1 - \frac{p}{\omega}\right)^{r-1} \frac{(1-\omega)}{\omega} f_{p|\eta}(\omega) dp d\omega, \\ &= \int_0^1 \int_0^\omega p^x \frac{(\omega-p)^{r-1}}{\omega^{r-1}} f_{p|\eta}(\omega) dp d\omega - \int_0^1 \int_0^\omega p^x \frac{(\omega-p)^{r-1} (1-\omega)}{\omega^{r-1}} f'_{p|\eta}(\omega) dp d\omega \\ &\quad + (r-1) \int_0^1 \int_0^\omega p^x \frac{(\omega-p)^{r-1} (1-\omega)}{\omega^r} f_{p|\eta}(\omega) dp d\omega. \end{aligned} \quad (\text{A4})$$

Finally, by interchanging the order of integration and rearranging components in (A4), we obtain

$$\begin{aligned}
\int_0^1 (1-p)^r p^x f_{p|r,\boldsymbol{\eta}}(p) dp &= \int_0^1 (1-p)^r p^x \left[\frac{1}{(1-p)^r} \int_p^1 \frac{(\omega-p)^{r-1}}{\omega^{r-1}} f_{p|\boldsymbol{\eta}}(\omega) d\omega \right] dp \\
&\quad - \int_0^1 (1-p)^r p^x \left[\frac{1}{(1-p)^r} \int_p^1 \frac{(\omega-p)^{r-1} (1-\omega)}{\omega^{r-1}} f'_{p|\boldsymbol{\eta}}(\omega) (\omega) d\omega \right] dp \\
&\quad + \int_0^1 (1-p)^r p^x \left[\frac{(r-1)}{(1-p)^r} \int_p^1 \frac{(\omega-p)^{r-1} (1-\omega)}{\omega^r} f_{p|\boldsymbol{\eta}}(\omega) d\omega \right] dp \\
&= \int_0^1 (1-p)^r p^x \left\{ \frac{1}{(1-p)^r} \int_p^1 \frac{(\omega-p)^{r-1}}{\omega^{r-1}} \left[1 + (r-1) \frac{(1-\omega)}{\omega} \right] f_{p|\boldsymbol{\eta}}(\omega) d\omega \right\} dp \\
&\quad - \int_0^1 (1-p)^r p^x \left[\frac{1}{(1-p)^r} \int_p^1 \frac{(\omega-p)^{r-1} (1-\omega)}{\omega^{r-1}} f'_{p|\boldsymbol{\eta}}(\omega) d\omega \right] dp,
\end{aligned}$$

which implies (7).

If $r \in (1, \infty)$, then one can use integration by parts to rewrite the second term on the right-hand side of (7) as

$$\frac{1}{(1-p)^r} \int_p^1 \frac{(\omega-p)^{r-1}}{\omega^{r-1}} \left[\frac{p(r-1)(1-\omega)}{(\omega-p)\omega} - 1 \right] f_{p|\boldsymbol{\eta}}(\omega) d\omega,$$

and substitute this expression to obtain (6). (Integration by parts cannot be used for $r \in (0, 1)$ because the resulting terms diverge to infinity at $\omega = p$.)

The uniqueness of $f_{p|r>1,\boldsymbol{\eta}}(p)$ follows from the identifiability of Negative Binomial mixtures for fixed r . If $f_{p|r<1,\boldsymbol{\eta}}(p)$ is a proper PDF, then its uniqueness follows in the same way. The existence of quasi-PDF solutions is shown by Theorem 3. ■

A.3 Proof of Theorem 3

For part (1), consider the limit of (7) as $p \rightarrow 0^+$:

$$\begin{aligned}
\lim_{p \rightarrow 0^+} f_{p|r<1,\boldsymbol{\eta}}(p) &= \lim_{p \rightarrow 0^+} \frac{1}{(1-p)^r} \left[(2-r) \int_p^1 \left(\frac{\omega-p}{\omega} \right)^{r-1} f_{p|\boldsymbol{\eta}}(\omega) d\omega \right. \\
&\quad \left. + (r-1) \int_p^1 \left(\frac{\omega-p}{\omega} \right)^{r-1} \omega^{-1} f_{p|\boldsymbol{\eta}}(\omega) d\omega - \int_p^1 \left(\frac{\omega-p}{\omega} \right)^{r-1} (1-\omega) f'_{p|\boldsymbol{\eta}}(\omega) d\omega \right] \\
&= 2-r + (r-1) \lim_{p \rightarrow 0^+} \int_p^1 \omega^{-1} f_{p|\boldsymbol{\eta}}(\omega) d\omega - \left[(1-\omega) f_{p|\boldsymbol{\eta}}(\omega) \Big|_0^1 + \int_0^1 f_{p|\boldsymbol{\eta}}(\omega) d\omega \right] \\
&= \lim_{p \rightarrow 0^+} \left[f_{p|\boldsymbol{\eta}}(p) + (r-1) \int_p^1 \omega^{-1} f_{p|\boldsymbol{\eta}}(\omega) d\omega \right] - r + 1. \tag{A5}
\end{aligned}$$

Clearly, $f_{p|r<1,\eta}(p)$ is a quasi-PDF with $\lim_{p \rightarrow 0^+} f_{p|r<1,\eta}(p) \leq \ell < 0$ in some neighborhood of 0 if and only if (A5) is negative; or equivalently,

$$\lim_{p \rightarrow 0^+} \int_p^1 \omega^{-1} f_{p|\eta}(\omega) d\omega \left[\frac{f_{p|\eta}(p)}{\int_p^1 \omega^{-1} f_{p|\eta}(\omega) d\omega} + r - 1 \right] < r - 1. \quad (\text{A6})$$

If $\lim_{p \rightarrow 0^+} f_{p|\eta}(p) = 0$, then (A6) must hold because $\lim_{p \rightarrow 0^+} \int_p^1 \omega^{-1} f_{p|\eta}(\omega) d\omega = E_{\omega|\eta} \left[\frac{1}{\omega} \right] > 1$. Moreover, if $0 < \lim_{p \rightarrow 0^+} f_{p|\eta}(p) < \infty$, then (A6) holds because $\lim_{p \rightarrow 0^+} \int_p^1 \omega^{-1} f_{p|\eta}(\omega) d\omega = \infty$. Finally, if $\lim_{p \rightarrow 0^+} f_{p|\eta}(p) = \infty$ (implying $\lim_{p \rightarrow 0^+} \int_p^1 \omega^{-1} f_{p|\eta}(\omega) d\omega = \infty$ as well), then (A6) is satisfied if

$$\begin{aligned} \lim_{p \rightarrow 0^+} \left[\frac{f_{p|\eta}(p)}{\int_p^1 \omega^{-1} f_{p|\eta}(\omega) d\omega} + r - 1 \right] < 0 \\ \iff \lim_{p \rightarrow 0^+} \frac{-p f'_{p|\eta}(p)}{f_{p|\eta}(p)} < 1 - r, \end{aligned}$$

where the last inequality follows from L'Hôpital's rule. Condition (A6) may or may not be true if $\lim_{p \rightarrow 0^+} f_{p|\eta}(p) = \infty$ and $\lim_{p \rightarrow 0^+} \frac{-p f'_{p|\eta}(p)}{f_{p|\eta}(p)} = 1 - r$, because the expression on the left-hand side of (A6) becomes indeterminate.

For part (2), we first note that $\lim_{p \rightarrow 0^+} f_{p|\eta}(p) = \infty$ and $\lim_{p \rightarrow 0^+} \frac{-p f'_{p|\eta}(p)}{f_{p|\eta}(p)} \geq 1 - r$ (because (7) would be a quasi-PDF by (1)(a) otherwise), and rewrite (7) as

$$f_{p|r<1,\eta}(p) = \frac{1}{(1-p)^r} \int_p^1 \left(\frac{\omega-p}{\omega} \right)^{r-1} \left\{ 1 - (1-\omega) \left[\frac{f'_{p|\eta}(\omega)}{f_{p|\eta}(\omega)} - \frac{(r-1)}{\omega} \right] \right\} f_{p|\eta}(\omega) d\omega. \quad (\text{A7})$$

Then, since the inequality

$$\frac{-p f'_{p|\eta}(p)}{f_{p|\eta}(p)} > 1 - r - \frac{p}{1-p}$$

is equivalent to

$$1 - (1-p) \left[\frac{f'_{p|\eta}(p)}{f_{p|\eta}(p)} - \frac{(r-1)}{p} \right] > 0,$$

it follows that the expression inside the curly brackets – and therefore the entire integral in (A7) – must be positive. ■

A.4 Proof of Theorem 4

Rewriting (8) with $r = 1$ yields

$$f_{X|r=1,p}^{(\text{NB})}(x) = \int_0^\infty f_{X|\lambda}^{(\text{P})}(x) f_{\lambda|r=1, \frac{1-p}{p}}^{(\Gamma)}(\lambda) d\lambda.$$

Substituting the right-hand side of this equation into

$$f_{X|\eta}(x) = \int_0^1 f_{X|r=1,p}^{(\text{NB})}(x) f_{p|\eta}(p) dp$$

then gives

$$\begin{aligned} f_{X|\eta}(x) &= \int_0^1 \left[\int_0^\infty f_{X|\lambda}^{(\text{P})}(x) f_{\lambda|r=1, \frac{1-p}{p}}^{(\Gamma)}(\lambda) d\lambda \right] f_{p|\eta}(p) dp \\ &= \int_0^\infty f_{X|\lambda}^{(\text{P})}(x) \left[\int_0^1 f_{\lambda|r=1, \frac{1-p}{p}}^{(\Gamma)}(\lambda) f_{p|\eta}(p) dp \right] d\lambda \\ &= \int_0^\infty f_{X|\lambda}^{(\text{P})}(x) f_{\lambda|\eta}(\lambda) d\lambda. \blacksquare \end{aligned}$$

A.5 Proof of Theorem 5

For part (A), consider

$$\begin{aligned} f_{X|b,c>0}^{(\text{ZY})}(x) &= \int_0^1 f_{X|r=1,p}^{(\text{NB})}(x) f_{p|b,c>0}^{(\Sigma_B)}(p) dp \\ &= \int_0^1 (1-p) p^x \frac{c(1-p^c)^b}{\Sigma_B\left(\frac{1}{c}, \frac{1}{c}, b\right)(1-p)} dp \\ &= \frac{c}{\Sigma_B\left(\frac{1}{c}, \frac{1}{c}, b\right)} \int_0^1 (p^c)^{x/c} (1-p^c)^b dp. \end{aligned} \tag{A8}$$

Substituting $q = p^c$ into the above integral allows us to rewrite (A8) as

$$\begin{aligned} &\frac{1}{\Sigma_B\left(\frac{1}{c}, \frac{1}{c}, b\right)} \int_0^1 q^{(x-c+1)/c} (1-q)^b dq \\ &= \frac{1}{\Sigma_B\left(\frac{1}{c}, \frac{1}{c}, b\right)} \mathbf{B}\left(\frac{x+1}{c}, b+1\right). \end{aligned}$$

For part (B), note that

$$\begin{aligned} f_{X|b,c \rightarrow 0}^{(\text{ZY})}(x) &= \int_0^1 f_{X|r=1,p}^{(\text{NB})}(x) f_{p|b,c \rightarrow 0}^{(\Sigma_B)}(p) dp \\ &= \int_0^1 (1-p) p^x \frac{(-\ln(p))^b}{\zeta(b+1)\Gamma(b+1)(1-p)} dp \\ &= \frac{1}{\zeta(b+1)\Gamma(b+1)} \int_0^1 p^x (-\ln(p))^b dp. \end{aligned} \tag{A9}$$

Then, using the substitution $t = -\ln(p)$ in the above integral, (A9) can be rewritten as

$$\begin{aligned}
& \frac{1}{\zeta(b+1)\Gamma(b+1)} \int_{\infty}^0 (e^{-t})^x t^b (-e^{-t}) dt \\
&= \frac{1}{\zeta(b+1)\Gamma(b+1)} \int_0^{\infty} (e^{-t})^{x+1} t^b dt \\
&= \frac{(x+1)^{-(b+1)}}{\zeta(b+1)} \int_0^{\infty} \frac{(x+1)^{b+1} t^b e^{-(x+1)t}}{\Gamma(b+1)} dt \\
&= \frac{(x+1)^{-(b+1)}}{\zeta(b+1)}. \blacksquare
\end{aligned}$$

A.6 Proof of Corollary 1

In parts (A)(1) and (A)(2), the functional forms follow immediately by replacing $f_{p|\eta}(p)$ by (12) in parts (2) and (3), respectively, of Theorem 2. In parts (B)(1) and (B)(2), the functional forms similarly follow by replacing $f_{p|\eta}(p)$ by (13) in parts (2) and (3), respectively, of Theorem 2.

The fact that $f_{p|r<1, b, c>0}(p) \leq \ell < 0$ for p in some neighborhood of 0 follows from condition (1)(a) of Theorem 3, since $\lim_{p \rightarrow 0^+} f_{p|b, c>0}^{(\Sigma_B)}(p) = \frac{c}{\Sigma_B(\frac{1}{c}, \frac{1}{c}, b)} \in (0, \infty)$. Likewise, $f_{p|r<1, b, c \rightarrow 0}(p) \leq \ell < 0$ in a neighborhood of 0 because $\lim_{p \rightarrow 0^+} f_{p|b, c \rightarrow 0}^{(\Sigma_B)}(p) = \infty$ and $\lim_{p \rightarrow 0^+} \frac{-p f_{p|b, c \rightarrow 0}^{(\Sigma_B)'}}{f_{p|b, c \rightarrow 0}^{(\Sigma_B)}}(p) = 0 < 1 - r$, thus satisfying the same condition of Theorem 3. \blacksquare

A.7 Proof of Corollary 2

For part (A), replacing $f_{p|\eta}(p)$ by (12) in Theorem 4 gives

$$\begin{aligned}
f_{\lambda|b, c>0}(\lambda) &= \int_0^1 \left(\frac{1-p}{p}\right) \exp\left(-\left(\frac{1-p}{p}\right)\lambda\right) \frac{c(1-p^c)^b}{\Sigma_B\left(\frac{1}{c}, \frac{1}{c}, b\right)(1-p)} dp \\
&= \frac{c}{\Sigma_B\left(\frac{1}{c}, \frac{1}{c}, b\right)} \int_0^1 \frac{1}{p} (1-p^c)^b \exp\left(-\left(\frac{1-p}{p}\right)\lambda\right) dp.
\end{aligned}$$

Substituting $y = \frac{1-p}{p}$ into this integral then yields the expression on the right-hand side of (14).

For part (B), replacing $f_{p|\eta}(p)$ by (13) in Theorem 4 gives

$$\begin{aligned}
f_{\lambda|b, c \rightarrow 0}(\lambda) &= \int_0^1 \left(\frac{1-p}{p}\right) \exp\left(-\left(\frac{1-p}{p}\right)\lambda\right) \frac{(-\ln(p))^b}{\zeta(b+1)\Gamma(b+1)(1-p)} dp \\
&= \frac{1}{\zeta(b+1)\Gamma(b+1)} \int_0^1 \frac{1}{p} (-\ln(p))^b \exp\left(-\left(\frac{1-p}{p}\right)\lambda\right) dp.
\end{aligned}$$

Substituting $y = \frac{1-p}{p}$ into this integral then yields the right-hand side of (15). \blacksquare

A.8 Proof of Corollary 3

In part (1), the functional form follows immediately by replacing $f_{p|\eta}(p)$ by

$$f_{p|a,b}^{(B)}(p) = \frac{1}{\mathbf{B}(a,b)} p^{a-1} (1-p)^{b-1} \quad (\text{A10})$$

in part (2) of Theorem 2. In parts (2) and (3), the functional form similarly follows by replacing $f_{p|\eta}(p)$ by (A10) in part (3) of Theorem 2.

To show that $f_{p|r<1,a,b}(p)$ is the unique mixing PDF when $r \geq a$, first note that $\lim_{p \rightarrow 0^+} f_{p|a<1,b}^{(B)}(p) = \infty$ and $\lim_{p \rightarrow 0^+} \frac{-p f_{p|a<1,b}^{(B)'}}{f_{p|a<1,b}^{(B)}} = 1 - a \geq 1 - r$. Then, since $\frac{-p f_{p|a<1,b}^{(B)'}}{f_{p|a<1,b}^{(B)}} = \frac{bp}{1-p} + 2 - a - \frac{1}{1-p} > 1 - r - \frac{p}{1-p}$ for all $p \in (0, 1)$, the result follows from condition (2)(a) of Theorem 3.

To show that $f_{p|r<1,a,b}(p) \leq \ell < 0$ for all p in some neighborhood of 0 when $r < a$, we must consider three cases: $a > 1$, $a = 1$, and $a < 1$. For $a > 1$ and $a = 1$, the result follows from condition (1)(a) of Theorem 3, since $\lim_{p \rightarrow 0^+} f_{p|a>1,b>0}^{(B)}(p) = 0$ and $\lim_{p \rightarrow 0^+} f_{p|a=1,b>0}^{(B)}(p) = b \in (0, \infty)$, respectively. For $a < 1$, the same condition of Theorem 3 applies, since $\lim_{p \rightarrow 0^+} f_{p|a<1,b}^{(B)}(p) = \infty$ and $\lim_{p \rightarrow 0^+} \frac{-p f_{p|a<1,b}^{(B)'}}{f_{p|a<1,b}^{(B)}} = 1 - a < 1 - r$. ■

A.9 Proof of Corollary 4

Replacing $f_{p|\eta}(p)$ by (A10) in Theorem (4) gives

$$\begin{aligned} f_{\lambda|a,b}(\lambda) &= \int_0^1 \left(\frac{1-p}{p} \right) \exp \left(- \left(\frac{1-p}{p} \right) \lambda \right) \frac{p^{a-1} (1-p)^{b-1}}{\mathbf{B}(a,b)} dp \\ &= \frac{1}{\mathbf{B}(a,b)} \int_0^1 p^{a-1} (1-p)^{b-1} \exp \left(- \left(\frac{1-p}{p} \right) \lambda \right) dp. \end{aligned}$$

Substituting $y = \frac{1-p}{p}$ into this integral then yields the expression on the right-hand side of (16). ■